THE ROLE OF NS1-BP IN INFLUENZA VIRUS REPLICATION

APPROVED BY SUPERVISORY COMMITTEE

Beatriz M.A. Fontoura, Ph.D.

Michael G. Roth, Ph.D.

Yuh Min Chook, Ph.D.

Nicholas K. Conrad, Ph.D.

DEDICATION

This thesis is dedicated to my family for their love and support.

THE ROLE OF NS1-BP IN INFLUENZA VIRUS REPLICATION

by

PEI-LING TSAI

DISSERTATION / THESIS

Presented to the Faculty of the Graduate School of Biomedical Sciences

The University of Texas Southwestern Medical Center at Dallas

In Partial Fulfillment of the Requirements

For the Degree of

DOCTOR OF PHILOSOPHY

The University of Texas Southwestern Medical Center at Dallas

Dallas, Texas

December, 2011

THE ROLE OF NS1-BP IN INFLUENZA VIRUS REPLICATION

PEI-LING TSAI, Ph.D.

The University of Texas Southwestern Medical Center at Dallas, 2011

BEATRIZ MA FONTOURA, Ph.D.

Influenza A viruses are negative-sense, segmented RNA viruses which cause about 500,000 deaths worldwide per year. Genomic studies have shown that the non-structural protein (NS1) of influenza A virus is a major virulence factor that is essential for pathogenesis. NS1 is a multifunctional protein localized in the nucleus and in the cytoplasm. In the cytoplasm, NS1 inhibits host signaling pathways that result in down-regulation of interferon expression and innate immune response. In the nucleus, NS1 represses host gene expression. I have shown that NS1

binds an mRNA complex containing NXF1/TAP, NXT/p15, Rae1, and E1B-AP5, which are key components of the mRNA export machinery. By targeting this complex, NS1 blocks host mRNA export, and cells become highly permissive to viral replication. Another intranuclear pool of NS1 was found to interact with a host protein termed NS1-BP, which has been suggested to play a role in pre-mRNA splicing. However, the functions and mechanisms of NS1-BP involved in influenza life cycle remain to be elucidated. To investigate the function of NS1-BP, I first identified its binding partners by immunoprecipitation followed by mass spectrometry. We found interactions of NS1-BP with viral polymerase complex and host RNA polymerase II indicating that NS1-BP has a role in regulating viral RNA transcription and replication. I further showed that low levels of NS1-BP led to a decrease in viral polymerase activity resulting in inhibition of virus replication. Thus, I identified NS1-BP as a novel pro-viral factor required for proper replication of influenza virus. Since NS1 is a key contributor to the virulence of influenza viruses, discovering the function of NS1 interacting partners has major implications for antiviral therapy.

TABLE OF CONTENTS

PRIOR PUBLICATIONS

Hsieh, M.M., Kuo, Y.C., **Tsai, P.L.**, and Chang, H.T. (2001). Optimizing separation conditions for polycyclic aromatic hydrocarbons in micellar electrokinetic chromatography. J Chromatogr A 924, 397-405

Tsai, P.L., Chen, C.H., Huang, C.J., Chou, C.M., and Chang, G.D. (2004) Purification and cloning of an endogenous protein inhibitor of carp nephrosin, an astacin metalloproteinase. J Biol Chem 279, 11146-11155

Satterly, N., **Tsai, P.L.**, van Deursen, J., Nussenzveig, D.R., Wang, Y., Faria, P.A., Levay, A., Levy, D.E., and Fontoura, B.M. (2007). Influenza virus targets the mRNA export machinery and the nuclear pore complex. Proc Natl Acad Sci U S A 104, 1853-1858

LIST OF FIGURES

LIST OF TABLES

LIST OF DEFINITIONS

ARA3: Aryl hydrocarbon-receptor associated protein 3

ARNT: AHR nuclear translocator

BACK domain: BTB-and C-terminal Kelch domain

BSA: bovine serum albumin

BTB/POZ domain: broad complex/tramtrack/bric-a-brac domain

CARD domain: caspase activation and recruitment domain

cDNA: complementary DNA

CMV promoter: cytomegalovirus promoter

CPSF: cleavage and polyadenylation specificity factor

Ct number: threshold cycle number

DAPI: 4',6-diamidino-2-phenylindole

DEAD box polypeptide: (Asp-Glu-Ala-Asp) box polypeptide

DEAE-Dextran: diethylaminoethyl dextran

DHX9: DEAH (Asp-Glu-Ala-His) box polypeptide 9

DMEM: Dulbecco's Modified Eagle Medium

dNTP: deoxyribonucleotide triphosphate

DTT: dithiothreitol

E1B-AP5: adenovirus early region 1B-associated protein 5

ECL: enhanced chemilumescent

EDTA: ethylenediaminetetraacetic acid

eIF2a: eukaryotic initiation factor 2

EMEM: Eagle's Minimum Essential Medium

EU: 5-ethynyl uridines

GAPDH: Glyceraldehyde 3-phosphate dehydrogenase

GST: glutathione S-transferase

HEPES: 4-(2-hydroxyethyl)-1-piperazineethanesulfonic acid

hnRNP: heterogeneous nuclear ribonucleoprotein

HPLC: high-performance liquid chromatography

HRP: horseradish peroxidase

Hsp90: heat shock protein 90

IFN-a/b: Interferon a and b

IgG: Immunoglobulin G

IKK: Inhibitors of NF-kB kinase

Influenza cRNA: viral complementary RNA

Influenza HA: haemagglutinin

Influenza M1: matrix protein M1

Influenza M2: matrix protein M2 (ion channel)

Influenza mRNA: viral messenger RNA

Influenza NA: neuraminidase

Influenza NEP/NS2: nuclear export protein/non-structural protein 2

Influenza NP: nucleoprotein

Influenza NS1: non-structural protein 1

Influenza PA: polymerase acid

Influenza PB1: polymerase basic 1

Influenza PB2: polymerase basic 2

Influenza RdRp: viral RNA-dependent RNA polymerase

Influenza svRNA: small regulatory viral RNA

Influenza vRNA: viral genome RNA

Influenza vRNP: viral ribonucleoprotein complex

IPTG: isopropyl-beta-D-thiogalactopyranoside

IRF-3: Interferon regulatory factor 3

ISG: interferon-stimulated genes

LB: lysogeny broth

LC/MS: liquid chromatography–mass spectrometry

M-MLV RT: Moloney Murine Leukemia Virus reverse transcriptase

MAVS: mitochondria antiviral signaling protein

MOI: multiplicity of infection

NF-kB: Nuclear Factor-KappaB

NFAR: nuclear factor associated with dsRNA

NLS: nuclear localization signals

NS1-BP: influenza virus NS1A binding protein

NXF1/TAP: Nuclear RNA export factor 1

OAS: 2'-5'-oligoadenylate synthetase

OD: optical density

p15/NXT: NTF2-like export protein 1

PABPII: poly(A) binding protein II

PARP: poly (ADP-ribose) polymerase

PBS-T: phosphate buffered saline with 0.05% tween 20

PBS: phosphate buffered saline

PCA: Phenol:Chloroform:Isoamyl Alcohol

PKR: protein kinase R

PMSF: phenylmethylsulfonyl fluoride

Pol II CTD: RNA polymerase II C-terminal domain

PVDF: polyvinylidene fluoride

qPCR: quantitative real time polymerase chain reaction

Rae1/mrnp41: RNA export 1 homolog

RdRp: RNA-dependent RNA polymerase

RIG-I: retinoic acid inducible gene-I

RIPA buffer: radioimmunoprecipitation assay buffer

RPL32: ribosomal protein L32

RT-PCR: reverse transcription polymerase chain reaction

SDS-PAGE: sodium dodecyl sulfate polyacrylamide gel electrophoresis

siRNA: small interfering RNA

SV40 promoter: Simian vacuolating virus 40 promoter

TBK1: TANK-binding kinase 1

TEMED: N,N,N',N'-tetramethylethane-1,2-diamine

TPCK: L-1-tosylamido-2-phenylethyl chloromethyl ketone

TRIM25: tripartite motif containing 25

VCP: valosin-containing protein

VRC: vanadyl-ribonucleoside complex

WBS: Williams-Beuren syndrome chromosomal region 16 protein

CHAPTER ONE

INTRODUCTION

1.1 Overview of influenza A virus

Influenza A virus belongs to the *Orthomyxoviridae* family of RNA viruses. It is an enveloped virus with a viral genome comprised of eight single-stranded, negative-sensed RNA segments encoding 11 or 12 proteins (Medina and Garcia-Sastre, 2011; Palese and Shaw, 2007). Among the viral genome, two segments generate spliced products: non-structural protein (NS1) and nuclear export protein (NEP/NS2) are encoded from the NS segment; matrix protein (M1) and ion channel (M2) are encoded from the M segment. Two glycoproteins haemagglutinin (HA) and neuraminidase (NA) and the viral polymerase complex PB1 (polymerase basic 1), PB2 (polymerase basic 2), PA (polymerase acid), and nucleoprotein (NP) are encoded from respective segments. In addition, N40 is a newly identified viral protein derived from the PB1 segment, whose function is unclear (Wise et al., 2009), and some viruses encode PB1-F2 protein, which is expressed from a different open reading frame within the PB1 segment and has been suggested to play a role in pro-apoptosis (Chen et al., 2001; Gibbs et al., 2003; Zamarin et al., 2005).

Influenza A viruses are divided into different subtypes based on the expression of the glycoproteins haemagglutinin (HA) and neuraminidase (NA) located on the surface of the viral coat. Currently, there are 16 HA and 9 NA subtypes identified in birds, and two subtypes H1N1 and H3N2 are found circulating in humans. Different influenza virus strains are named based on the virus types (influenza A, B, or C), the host (omitted, if human), place of isolation, the number of isolation, the year of isolation, and the subtypes of HA and NA in the case of influenza A virus. For instance, World Health Organization reports that the flu vaccine for 2011-2012 is against the virus strains A/California/7/2009 (H1N1), A/Perth/16/2009 (H3N2), and B/Brisbane/60/2008 (Palese and Shaw, 2007; Taubenberger and Kash, 2010).

Influenza A virus is a zoonotic pathogen, which circulate in several animals and can be transmitted to humans. The antigenic evolution of the surface glycoproteins HA and NA is driven through antigenic drift, which is a gradual change in genotype due to the pressure of the antibody-mediated immune selection. Most newly identified seasonal strains are selected by this mechanism and are characterized by several changes in amino acids of HA and NA. However, more dramatic changes could result from antigenic shift. In this case, a single cell that is infected with two

different strains of influenza A viruses may result in viral genome reassortment or mixing, which leads to the generation of a novel strain with new subtypes of HA or NA. Most influenza pandemics are thought to have arisen in this manner (Medina and Garcia-Sastre, 2011; Wright et al., 2007). Influenza A virus caused several pandemics in the past one hundred years. The most severe pandemic occurred in 1918 killing ~50 million people around the world (Johnson and Mueller, 2002). Recently, a novel swine-origin influenza A strain emerged in 2009 and to date is responsible for more than 180,000 deaths worldwide (Medina and Garcia-Sastre, 2011). Understanding the mechanisms responsible for the transmission between species and the rapid mutation rates will help us predict or fight pandemics in the future.

1.2 Virion structure

Influenza A virus is a spherical or filamentous virus with a diameter of approximately 100 nm (Figure 1). Projecting from the viral surface are two glycoproteins, haemagglutinin (HA) and neuraminidase (NA). Haemagglutinin (HA) is responsible for determining the host species, as it recognizes terminal α-2,3-linked or α-2,6-linked sialic acids on the host

receptor. Avian viruses prefer the α-2,3-linked sialic acid, and human viruses prefer to bind α-2,6-linked sialic acid. In contrast, neuraminidase (NA) functions in destroying the interaction between sialic acid-containing receptor and viral membrane during the virus budding. The ratio of HA to NA on the virus surface is approximately four HA to one NA. M2 protein is an ion channel embedded on the surface. It conducts the entry of protons into the virion during endocytosis, which facilitates the uncoating of the viral genome. Underneath the lipid bilayers, there is a layer composed of matrix protein M1 interacting with surface proteins and holding the viral ribonucleoprotein complexes (vRNPs). The vRNPs are the core of viral particles and are comprised of viral polymerase complex and RNAs. Influenza viral RNA is wrapped around nucleoprotein (NP) and forms a panhandle structure with the complementary base-pairing between the 5' and 3'-untranslated regions. The terminal sequences of the 5' and 3' UTR are conserved in all viral segments, and the viral polymerase complex localizes at the end of the panhandle structure, holding both 5' and 3' ends of the RNA. Influenza viral polymerase is a heterotrimeric complex consisting of PB1, PB2, and PA subunits. PB1 possesses the RNA polymerase activity, PB2 binds to the cap-structure of cellular mRNA, and PA has recently been shown to have endonuclease activity that is required

for the cap-snatching mechanism (discussed below). The nuclear export protein (NEP/NS2) helps export vRNP out of the nucleus and is included within the virion. However, the non-structural protein (NS1) does not exist in the virion; it is expressed after infection (Palese and Shaw, 2007), and (Medina and Garcia-Sastre, 2011).

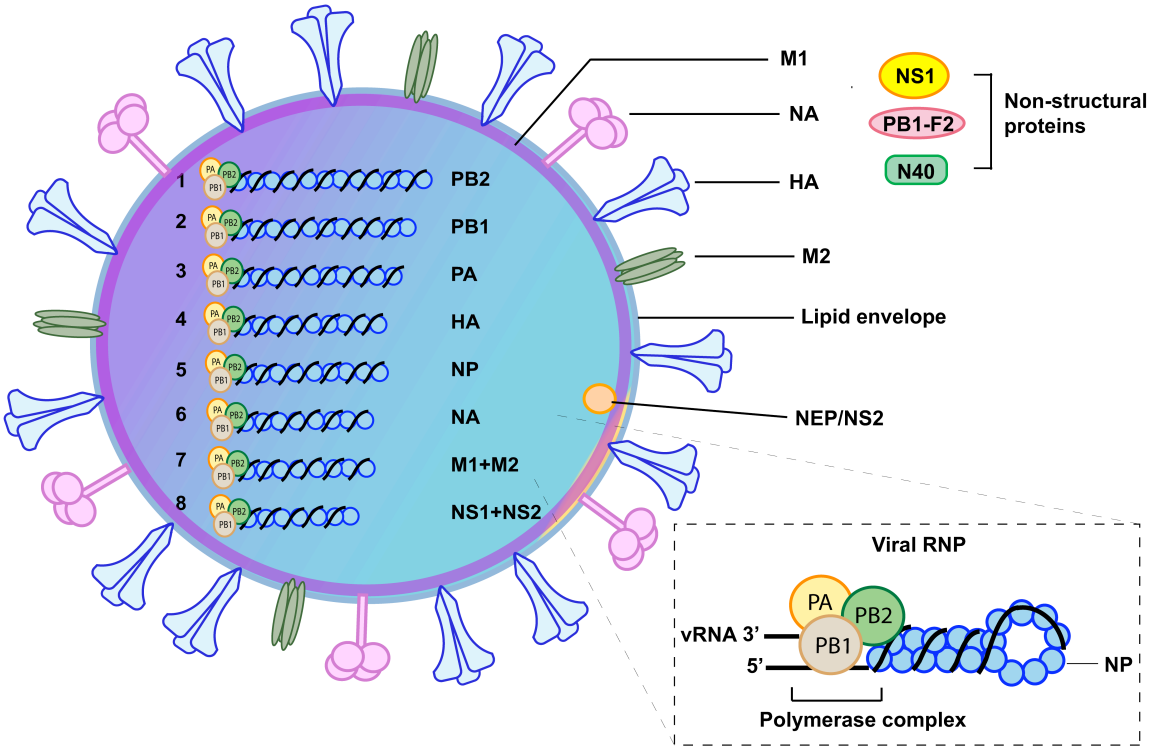

Figure 1. Influenza A virion structure
Influenza A virus consists of eight single-strand, segmented RNAs, encoding 11 or 12 proteins. Two of these segments generate spliced products: Matrix protein (M1) and the ion channel (M2) are encoded from the M segment; non-structural protein (NS1) and nuclear export factor (NEP/NS2) are encoded from the NS segment. Sialic acid-binding protein (HA), sialic acid-destroying enzyme (NA), nucleoprotein (NP), and viral polymerase complex (PB1, PB2, and PA) are encoded from the respective segments. N40 is a newly identified ptotein expressed by the PB1

segment; the function is unclear. Some viruses encode PB1-F2 that is derived from another ORF in the PB1 segment. Each RNA segment is coated with nucleoprotein (NP), and the viral polymerase complex is bound to the panhandle structure formed by the 5' and 3'-UTR of the viral RNA. This figure was adapted from the following references (Medina and Garcia-Sastre, 2011; Nagata et al., 2008).

Currently, several compounds targeting viral proteins have been identified and are used as inhibitors of influenza virus replication. Amantidine and rimantidine are known as M2 channel blockers, which interfere with membrane fusion and inhibit the uncoating of the viral genome (Pinto and Lamb, 1995). Oseltamivir and Zanamivir are inhibitors of the neuraminidase (Oxford et al., 2004; Oxford et al., 2003). In addition to the viral surface proteins, viral polymerase complex has recently been considered as ideal targets, which led to the development of several compounds. For example, Nucleozin and its analogue target the viral protein NP and cause cytoplasmic aggregations of NP (Kao et al., 2010; Su et al., 2010). The 2,4-diketobutanoic acid and its analogue target the PA (Hastings et al., 1996; Nakazawa et al., 2008; Tomassini et al., 1994). Favipiravir (T-705) has been shown to inhibit RNA viruses *in vitro* and acts as nucleoside analogue that is converted into the active form (T-705RTP) by cellular enzymes (Furuta et al., 2002; Furuta et al., 2005). Recently, our laboratory identified a naphthalimide, which acts on the host cell to

increase the expression of the mTORC1 inhibitor REDD1 resulting in down-regulation of influenza virus protein expression (Mata et al., 2011).

1.3 Overview of influenza A viral life cycle

Influenza A virus initiates infection by attaching to host surface receptors via its HA protein and then is internalized through endocytosis (Figure 2). Viral endocytosis has been thought to occur through clathrin-mediated endocytosis. However, a recent study found that the viruses also enter cells through a non-clathrin, non-caveolin dependent pathway (Mercer et al., 2010; Sieczkarski and Whittaker, 2002). HA protein is not only important for virus attachment but also for the viral genome uncoating. For a virus to become infectious, HA must be cleaved and activated by cellular trypsin-like proteases prior to endocytosis. HA_0 is the uncleaved form, which does not have infectious activity. After protease processing, HA_0 is cleaved into HA_1 and HA_2, which remain linked together at the viral surface by disulfide bonds. As the clathrin-coated vesicles traffic to endosome, the low pH (pH 5.0-6.0) induces HA_2 to expose the N-terminal fusion peptide that inserts into endosome membrane and then causes membrane fusion. Meanwhile, low pH also activates the M2 channel that

conducts proton influx into the virion, which disrupts the interactions between vRNPs and matrix protein M1, resulting in the release of the viral genome into the cytoplasm. Viruses with HA cleavage site defect cannot replicate due to the failure of uncoating the viral genome (Palese and Shaw, 2007; Stegmann, 2000).

Influenza virus replication depends on cellular factors in the nucleus, so the released viral ribonucleoproteins (vRNPs) have to be imported to the nucleus. All components of vRNPs (PB1, PB2, PA, and NP) have nuclear localization signals (NLS), but it has been shown that the NLS of NP is necessary and sufficient for nuclear import (Cros et al., 2005). The nuclear import process is mediated by karyopherin receptors. The karyopherin α directly binds to the NLS of NP and recruits karyopherin β, and the whole complex is then docked and transported through nuclear pore complex. Influenza virus has negative-sensed RNA, which is defined as complementary to mRNA and is not the template for translation (Baltimore, 1971). Therefore, within the nucleus, viral RNA-dependent RNA polymerase uses vRNA as a template to transcribe two types of positive-sensed RNA, messenger RNA (mRNA) and complementary RNA (cRNA). Viral mRNA is exported and translated in the cytoplasm. After translation, viral proteins required for vRNP assembly are further imported to the

nucleus. On the other hand, the viral polymerase uses cRNA as template to replicate more progeny vRNA; the newly synthesized vRNPs are then exported to cytoplasm for packing. Two viral proteins are involved in vRNP export process. The current model proposed that M1 interacts with vRNP and NEP/NS2; then the NEP/NS2 recruits the nuclear export receptor Crm1 to direct nuclear export of the complex. Interestingly, the site on M1 where NEP/NS2 binds is the nuclear localization signal of M1, so this suggests that NEP/NS2 might mask the NLS of M1 to prevent it from being transported back to the nucleus (Akarsu et al., 2003; Palese and Shaw, 2007).

Viral surface proteins HA, NA, and M2 are transported to the cell membrane through the trans-Golgi network. At the cell membrane, M1 facilitates the formation of the outward curvature of the cell membrane, and neuraminidase (NA) helps release the viral particles by disrupting the interaction between viral envelope and cellular sialic acids (Nayak et al., 2004; Schmitt and Lamb, 2005). Recently, ion channel M2 is shown to mediate the final step of budding. M2 localizes at the neck of the budding viral particle, and the M2 protein mutation results in the failure of viral membrane scission (Rossman et al., 2010).

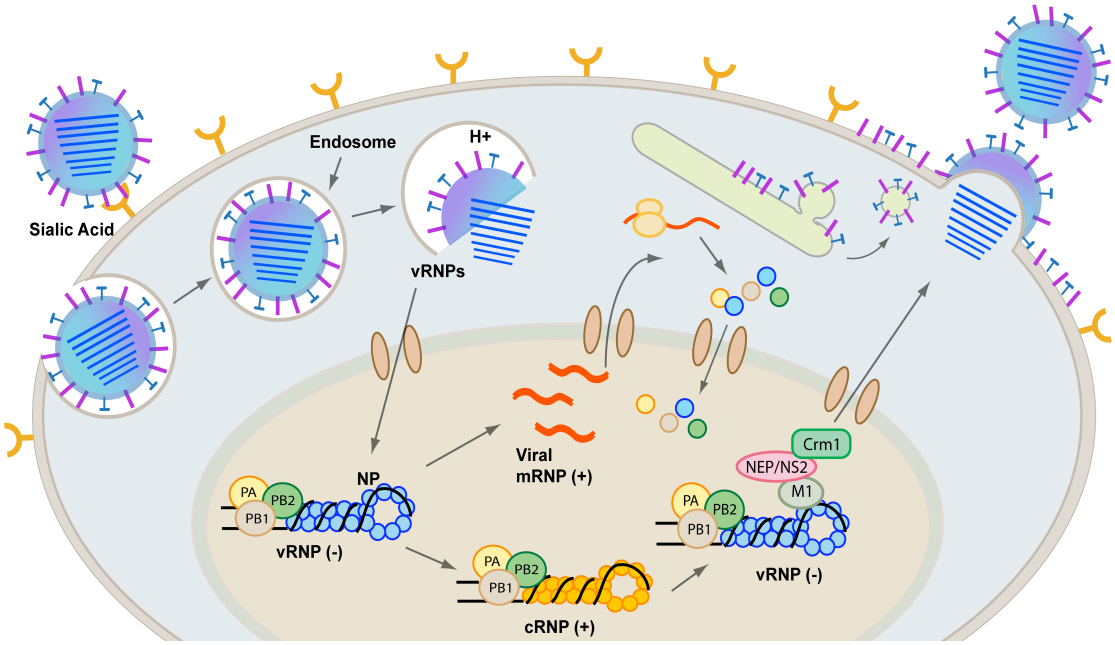

Figure 2. Influenza A virus life cycle.
Influenza A virus initiates the infection by attaching to sialic acids on the host cell via its HA protein and then enters the cell through endocyotsis. The low pH environment triggers the membrane fusion between viral envelope and endosomal membrane, which leads to the release of the viral genome. The vRNPs are then transported to the nucleus and transcribes two positive-sensed RNAs, mRNA and cRNA. Viral mRNA is exported to the cytoplasm for translation. Viral proteins required for vRNP assembly are further imported into the nucleus. On the other hand, cRNA is used as a template for producing more progeny vRNA. The newly synthesized vRNP is exported to the cytoplasm for packing via the Crm1-dependent pathway, assisted by M1 and NEP/NS2. Viral membrane proteins HA, NA, and M2 are translocated to the cell membrane through trans-Golgi network. At the plasma membrane, M1 helps with viral particle formation, then the budding occurs, and NA releases the virus by destroying the interaction between sialic acid and the receptor. This figure was adapted from the following references (Medina and Garcia-Sastre, 2011; Nagata et al., 2008).

1.4 Viral transcription and replication

As mentioned in the previous section, influenza virus RNA contains 5' and 3' UTR that forms a panhandle structure through the complementary sequence at the terminal of 5' and 3' ends of vRNA. This panhandle structure acts as a promoter for viral RNA-dependent RNA polymerase (RdRp) to dock (Brownlee and Sharps, 2002; Desselberger et al., 1980; Flick et al., 1996; Neumann and Hobom, 1995)(Figure 1). Viral transcription is dependent on the cellular RNA polymerase II, because it needs to access the cap-structure of host mRNA. To initiate transcription, PB2 recognizes the cap structure, PA cleaves a fragment about 10-13 nucleotides from the 5'-cap and anneals this primer to the 3'-end of vRNA, and PB1 performs the elongation. The process of stealing the 5'-cap from host mRNA is called cap snatching (Dias et al., 2009; Fechter et al., 2003; Guilligay et al., 2008; Plotch et al., 1981; Yuan et al., 2009) (Figure 3).

As for the polyadenylation, cellular mRNA contains poly(A) signal AATAAA in the 3'-mRNA, which is recognized and processed by the cleavage and polyadenylation specificity factor (CPSF) and poly(A) polymerase (Chan et al., 2011). However, the influenza virus genome does not include this element. Instead, the viral polymerase generates the

poly(A) tail based on five to seven continuous uracil at the 5'-end of vRNA. The vRNA is threaded in the 3' to 5' direction during transcription, when RdRp reaches the poly(U) region at the 5'-vRNA, the steric hindrance makes the RdRp stutter and slip between the template and nascent viral mRNA, which eventually results in the generation of repeated poly(A) sequences (Poon et al., 1999; Poon et al., 1998; Zheng et al., 1999). The poly(A) tail of viral mRNA is crucial for nuclear export; previous study showed that the replacement of poly(A) tail to poly(U) causes the failure of mRNA export (Poon et al., 2000).

In contrast to viral mRNA transcription, influenza genome replication is a primer-independent process. To initiate the replication, the RdRp first synthesizes a complementary strand (cRNA) by terminal initiation, and then this cRNA intermediate is used as a template for producing more progeny vRNAs (Figure 3). Unlike viral mRNA, cRNA is a complete full-length copy of the viral genome, and it does not contain a poly(A) tail. Since both mRNA and cRNA are derived from the same template (vRNA) and produced by the same polymerase complex, how does the RdRp overcome the steric hindrance and avoid making the poly(A) tail during cRNA generation? Recent studies proposed a mechanism that might reconcile this paradox. Influenza A virus has been known to generate a

small regulatory viral RNA termed svRNA that is segment specific and consists of 22-27 nucleotides corresponding to the sequence at 5'-end vRNA (Perez et al., 2010; Umbach et al., 2010). This study suggested that viral RdRp incorporates the svRNA when it undergoes cRNA synthesis. This mechanism allows svRNA to reconstitute the promoter *in trans*, allowing the RdRp to access the genomic end and makes a full-length copy of the vRNA. In contrast, during viral mRNA synthesis, the lack of svRNA allowed RdRp to remain *in cis* of 5'-vRNA, in which the RdRp encounters the steric hindrance and results in the generation of the poly(A) tail (Perez et al., 2010). This mechanism suggested that RdRp might recruit different elements into the complex to help itself adapt to different tasks.

As influenza virus enters the cell, it requires viral proteins to perform the functions; therefore, viral transcription is more dominant than replication in early post infection. However, how does the virus determine when to switch from transcription to replication? Unlike viral mRNA, virus vRNA and cRNA are coated with NP and RdRp, and one model has been proposed that the free form of NP (not bound to RNP) is responsible for switching the gear (Hay et al., 1977). When a cell accumulates enough NP proteins, this signals that the virus is ready for progeny replication and

then starts cRNA synthesis. Several pieces of evidences supports this model such as NP has been known to be required for full-length cRNA synthesis, suggesting that it stabilizes cRNA intermediates (Beaton and Krug, 1986). Furthermore, virus with temperature-sensitive NP shows the defects in cRNA synthesis but not in viral mRNA transcription. In this model, the concentration of NP determines whether the virus starts the replication cycle. Alternatively, as mentioned earlier, the svRNA is generated about 8-10 hours post infection and is associated with RdRp, which also provides another possible mechanism contributing to the switch. Currently, a new model is proposed, and it argues about the existence of a switch mechanism. Instead, it proposed that the incoming RdRp makes both viral mRNA and cRNA, but before the cell synthesizes enough pools of new synthesized NP and RdRp, the cRNA is degraded. Therefore, in early post infection, it is natural to have a bias toward transcription rather than replication (Vreede et al., 2004). The detailed mechanisms involved in the coordination between viral transcription and replication remain to be elucidated.

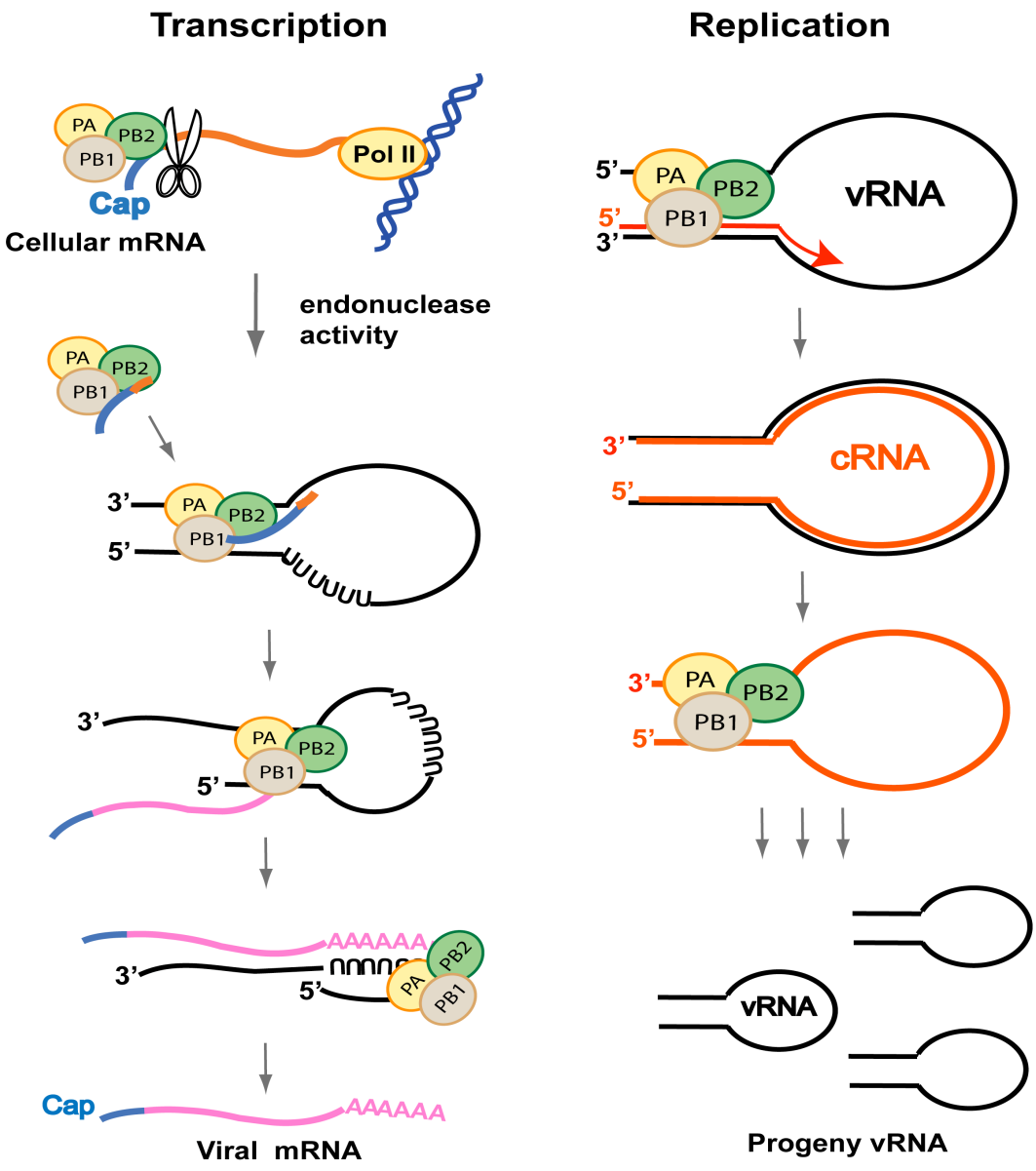

Figure 3. Transcription and replication of influenza virus.
Influenza virus initiates transcription using the cap-containing oligonucleotides derived from cellular mRNAs. PB2 binds to the cap structure and PA cleaves the site at 10-13 nucleotides away form the cap. Then PB1 elongates the capped-primer. When viral polymerase complex reaches the poly(U) region of the 5'-vRNA, the steric hindrance cause the polymerase stutters and slips between the nascent mRNA chain and the

template, which results in the synthesis of poly(A) tail on the nascent mRNA. In contrast to transcription, viral genome replication is a primer-independent process. Viral polymerase complex first synthesize a complementary RNA (cRNA), a full-length copy of vRNA, and use cRNA as a template to make more progeny vRNA. This figure is adapted from the reference (Nagata et al., 2008).

1.5 The multifunctional NS1 protein

When viruses enter cells, they trigger the host innate immune system that is responsible for establishing the anti-viral state by preventing infection in neighboring uninfected cells. Type I interferon (IFN-α/β) are cytokines secreted by cells in response to viral infection, which up-regulates the expressions of many interferon-stimulated genes (ISG) against viral replication (Randall and Goodbourn, 2008). Though host cells have such powerful mechanisms to inhibit virus spread, however, viruses have evolved sophisticated ways to counteract it and fulfill their life cycle. For instance, influenza A non-structural protein (NS1) has been known as such an antagonist of host immunity. In a previous study, viruses without NS1 (delNS1 mutant) were only able to replicate well in IFN-deficient system like Vero cells. Moreover, when mutant virus (delNS1) infected IFN-competent cells, the cells expressed 5 to 10 fold more IFN-α/β compared to cells infected with wild type virus, suggesting that NS1 is the

key factor to suppress cellular IFN-α/β expression (Garcia-Sastre et al., 1998). Recently, the mechanisms of how NS1 antagonizes the IFN-α/β pathway have been identified, in which NS1 targets RIG-I, a cytoplasmic pathogen sensor (Guo et al., 2007; Mibayashi et al., 2007; Opitz et al., 2007). RIG-I is a RNA-helicase and recognizes viral RNA harboring 5'-triphosphate (Hornung et al., 2006; Pichlmair et al., 2006). Upon activation with viral RNA, RIG-I undergoes conformation change and exposes the N-terminal CARD domain (caspase activation and recruitment domain), which interacts with the CARD domain of MAVS (mitochondria antiviral signaling protein). This interaction triggers the MAVS proteins at the mitochondria outer membrane to form the prion-like aggregates, which activate the cytosolic kinases IKK and TBK1 and results in the activation of the transcription factors NF-κB and IRF-3, eventually leading to the induction of type I interferon (Hou et al., 2011). Another recent study further reveals that NS1 interacts with TRIM25, an E3 ubiquitin ligase, which mediates the K63-ubiqutination in the N-terminal CARD domain of RIG-I. This modification is crucial for the activation of the downstream MAVS signaling pathway. By binding to TRIM25, NS1 abolishes the ubiquitination of RIG-I, leading to the inhibition of IFN-α/β production (Gack et al., 2009).

NS1 also blocks the functions of two cytoplasmic antiviral proteins, protein kinase R (PKR) and 2'-5'-oligoadenylate synthetase (OAS) (review in (Hale et al., 2008)) (Min and Krug, 2006; Min et al., 2007). PKR is activated by viral double strand RNA. Once activated, it phosphorylates translation initiation factor 2α (eIF2α), which ceases cellular and viral protein translation (Garcia et al., 2006). NS1 blocks PKR functions by several mechanisms. Since PKR is upregulated by IFN-α/β, NS1-induced inhibition of IFN-α/β expression indirectly reduces PKR level in infected cells. The N-terminal domain (1-73 amino acids) of NS1 is an RNA-binding domain. *In vitro* experiments suggest that NS1 might compete for dsRNA binding and sequester dsRNA from PKR (Hatada et al., 1999; Lu et al., 1995). However, this mechanism is challenged by later studies, which shows the NS1 with defective RNA-binding domain successfully blocks the PKR function upon dsRNA activation. Alternatively, NS1 has been shown to directly interact with PKR, which blocks the release of PKR auto-inhibition (Li et al., 2006). By inhibiting PKR function with NS1, viral translation is allowed to proceed.

The interferon-stimulated genes (ISG) encode proteins that mediate the interferon effect. Among these, the enzyme 2'-5'-oligoadenylate synthetase (OAS) is highly expressed. The 2'-5'-oligoadenylate synthetase

(OAS) is activated by viral dsRNA, which polymerizes ATP to 2'-5'-oligoadenylate and forms a chain. This chain activates a latent ribonuclease, RNaseL. The activated RNaseL inhibits virus replication by degradating viral RNA (Silverman, 2007). By competing out the dsRNA with its RNA-binding domain, NS1 disrupts this anti-viral strategy (Min and Krug, 2006)

NS1 is also in the nucleus at early stages of infection and it is then localized both in the nucleus and cytoplasm at later stages. In addition to the interferon pathway, NS1 also alters several cellular functions in the nucleus. Influenza virus has been known to inhibit host mRNA export, and this effect may be mediated through two mechanisms. NS1 has been shown to associate with CPSF30 and poly(A) binding protein II (PABPII) complex, which interrupts the processing of 3'-end poly(A) tail and results in the failure of host mRNA export (Chen et al., 1999; Nemeroff et al., 1998). More recently, I showed that NS1 forms an inhibitory complex, consisting of NXF1/TAP, p15/NXT, Rae1/mrnp41, and E1B-AP5, which are major constitutes of mRNA export machinery and mediate about 70% of cellular mRNA export. By targeting this machinery, NS1 blocks the bulk host mRNA export and translation, allowing the virus to use the translational machinery for its own replication (Satterly et al., 2007). As

mentioned above, viral RNA is exported from the nucleus through the Crm-1 dependent pathway; therefore, viral RNA export is likely not affected by NS1-induced blockage. In the nucleus, NS1 also interacts with other proteins such as nucleolin and NS1-BP, but the functions of these interactions remain unclear. In this study, I investigated the roles of NS1-BP in virus replication.

1.6 Overview of NS1-BP

Human NS1-BP protein consists of 642 amino acids and contains four major functional domains (Dunham et al., 2006). BTB/POZ (broad complex/tramtrack/bric-a-brac) domain mediates protein homo- or heterodimerizations, which has been found in some transcription regulators (Zollman et al., 1994). Moreover, the BTB/POZ domain has been shown to function as a substrate-specific adaptor of Cullin3 ubiquitin E3-ligase (Geyer et al., 2003; Pintard et al., 2003; Xu et al., 2003). At the C-terminus, NS1-BP contains 6 kelch repeats made up of 50 amino acids that form a β-propeller structure, which regulates protein-protein interaction. Like most BTB-Kelch proteins, NS1-BP also contains a conserved BACK (BTB-and C-terminal Kelch) domain, which has been

suggested to facilitate its interaction with the Cullin-3 ubiquitin ligase (Stogios and Prive, 2004). The last region does not show significant similarity to any known domains in the database so is designated as intervening region (IVR) (Dunham et al., 2006).

NS1-BP was cloned and identified as an interacting partner of the influenza virus non-structural protein (NS1) in a yeast two-hybrid screen. Most NS1-BP localizes in the nucleus and has been shown to co-localize with the spliceosome assembly factor (SC35) in speckles. Upon influenza virus infection, NS1-BP does not concentrate in the speckles; instead, it redistributes throughout the nucleoplasm. Using the truncated NS1-BP with *in vitro* splicing assay, the authors showed that the pre-mRNA splicing is inhibited by the truncated NS1-BP, suggesting that NS1-BP may play a role in pre-mRNA splicing (Wolff et al., 1998).

NS1-BP is also known as Ah-receptor associated protein 3 (ARA3). Aryl hydrocarbon receptor mediates xenobiotic metabolism by up-regulating the expression of detoxified enzymes such as cytophromes P450. Toxic materials like dioxin are potent agonists of this receptor. In the absence of ligand, the Ah receptor stays in the cytoplasm and is complexed with heat shock protein 90 (Hsp90) and cochaperone ARA9 (Carver et al., 1994). However, after ligand binding, it translocates to the

nucleus and dimerizes with protein AHR nuclear translocator (ARNT) (Carver et al., 1994). NS1-BP binds to AHR and regulates the signaling pathway, but the detail mechanisms remain unknown.

Another study indicated that NS1-BP interacts with alpha-enolase/MBP-1 that is identified as a binding protein of the c-myc promoter, and NS1-BP binding enhances the inhibitory effect on c-myc transcription controlled by MBP-1 (Perconti et al., 2007).

To date, there is little published information about NS1-BP. The murine analogue of NS1-BP is named Nd1 and encodes two isoforms generated from alternative splicing, named Nd1-L and Nd1-S, respectively (Kang et al., 2001). Nd1-L contains the BTB domain and the kelch domain, whereas Nd1-S has only the BTB domain. Nd1-L is expressed in all tissues, and it has been suggested to stabilize actin filaments (Sasagawa et al., 2002). Overexpression of Nd1-L delays cell proliferation by affecting cytokinesis, and this function is further investigated in cancer metastasis. Nd1-L siRNA-depletion promotes metastasis; however, overexpression of Nd1-L suppresses metastasis. Furthermore, increased levels of Nd1-L inhibit the small GTPases of the Rho family, such as Rac, Rho, and cdc42. Therefore, Nd1-L is suggested to play a role in cancer metastasis by regulating the dynamics of the actin cytoskeleton (Ohta et al., 2010). Nd1-

S is localized in the nucleus in a speckled-like pattern, and overexpression of Nd1-S causes defects in cell cycle progression, in which cells are stalled at the G1/S phase (Inoue et al., 2005). As mouse has two analogues of human NS1-BP, it is not yet clear that whether human NS1-BP adopts the similar functions.

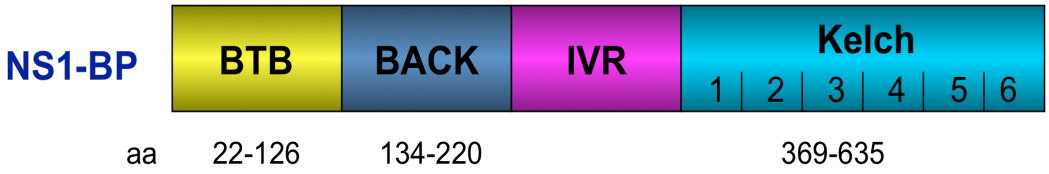

Figure 4. The diagram depicts the functional domains of NS1-BP. NS1-BP full length includes 642 amino acids. It contains a BTB domain from amino acids 22-126, followed by the BACK domain from amino acids 134-220. There are 6 kelch repeats at the C-terminal from amino acids 369-635. The IVR region is the sequence that does not match any known protein domain. The domain information is from the reference (Dunham et al., 2006)

1.7 Project specific aims

NS1-BP was first identified in 1998 and has been known as an interacting partner of the influenza A non-structural protein (NS1). However, it is unclear whether NS1 targeting to host protein NS1-BP is to inhibit the cellular functions or to benefit virus replication. To uncover functions of NS1-BP in the context of the influenza virus life cycle, I pursued the following specific aims:

Aim1: To identify the binding partners of NS1-BP

Aim2: To determine the role of NS1-BP in influenza virus replication

Aim3: To uncover the mechanisms by which NS1-BP regulates the influenza virus life cycle.

CHAPTER TWO

MATERIALS AND METHODS

2.1 Cells and Virus

Human lung adenocarcinoma epithelial cells (A549) were cultured in RPMI 1640 media (Invitrogen) supplemented with 10% heat-inactivated fetal bovine serum (Invitrogen), 100 units/mL penicillin, and 100 μg/mL streptomycin. HeLa cells and Madin Darby canine kidney cells (MDCK) were cultured in DMEM media (Invitrogen) containing the same amount of serum and antibiotics described above. All cells were maintained at 37°C with 5% CO_2.

Influenza virus (A/WSN/33) was a kind gift from Dr. Adolfo García-Sastre (Mount Sinai School of Medicine, NY). Viruses were propagated in MDCK cells. In brief, MDCK cells ($2x10^7$) were seeded into a 15 cm dish. At the second day, cells were washed in PBS and infected with viruses at multiplicity of infection (MOI) of 0.001 in 2.5 mL of infection media [EMEM (30-2003, ATCC), 10 mM HEPES, 0.2% BSA, 100 units/mL penicillin, 100 μg/mL streptomycin, and 0.5 μg/mL TPCK-treated trypsin]. After one hour of adsorption, cells were washed with PBS twice, overlaid with 10 mL

infection media, and incubated until viral cytopathicitiy was observed (about 36 hours). Supernatants were harvested, centrifuged at 1000xg for 10 min, aliquotted, and stored in -80°C. Virus titer was determined by plaque assay. Infection of A549 cells was similar to MDCK cells described above, except that the infection media did not contain TPCK-treated trypsin.

2.2 Plaque assay

The day before the assay, MDCK cells were seeded into 6-well plates at a density of $5x10^5$ cells/well. Ten-fold serial dilutions of each sample (from 10^{-1} to 10^{-7}) were prepared in 400 μL PBS containing 100 units/mL penicillin, 100 μg/mL streptomycin, 0.2% BSA, 0.9 mM $CaCl_2$, and 1.05 mM $MgCl_2$. Cells were infected with 300 μL of each diluted fraction. After one hour of adsorption, inoculums were removed, and cells were overlaid with 2 mL of agar mixture [1X EMEM (Lonza), 0.6% agar (Nobel Agar, Difco Microbiology), 100 units/mL penicillin, 100 μg/mL streptomycin, 2 mM L-glutamine, 0.2% bovine serum albumin (BSA), 10 mM HEPES, 0.22% sodium bicarbonate, 0.01% DEAE-Dextran, and 0.5 μg/mL TPCK-treated trypsin]. Plates were incubated at 37°C with 5% CO_2 for 48 hours.

After 2 days, cells were fixed by adding 2 mL of 2% formaldehyde on the top of the agar and incubated at room temperature for 1 hour. After removal of the agar, monolayers were stained with 0.1% crystal violet prepared in 0.25% methanol, and the plaques were counted.

2.3 Plasmids

Full-length cDNA clone of human NS1-BP (NM_006469.4) was purchased from OriGene Technologies, Inc. (Rockville, MD) and subcloned into the *Sal* I and *Not* I sites of expression vector pGEX-4T-2 (GE Healthcare). Influenza mini-genome reporter construct was kindly provided by Dr. Megan Shaw (Mount Sinai School of Medicine, NY) (Hoffmann et al., 2008). In brief, firefly luciferase gene was amplified by PCR, and 5' and 3'-cRNA promoter derived from influenza (A/WSN/33) NP segment were incorporated into two ends of the luciferase gene. The product was then cloned into a pPol I plasmid, in which the luciferase gene was in negative-sensed orientation. Constructs pcDNA-PB1, pcDNA-PB2, pcDNA-PA, and pcDNA-NP were gifts from Dr. Ervin Fodor (University of Oxford, United Kingdom). The minigene CD1 and CD9 constructs were gifts from Dr. Kristen Lynch (University of Pennsylvania, PA), and the

information of theses constructs were previously described (Rothrock et al., 2003).

2.4 Antibodies

GST-tagged full-length NS1-BP was used as an antigen to develop polyclonal antibodies in rabbits (Cocalico Biologicals, Reamstown, PA). The specific antiserum was purified by affinity chromatography (Bar-Peled and Raikhel, 1996) with some modifications. In brief, GST and full-length GST-NS1-BP were expressed in bacteria strain BL21(DE3) and purified by glutathione-Sepharose 4B beads (17-0756-01, GE Healthcare, Piscataway, NJ). Without elution, protein GST and GST-NS1-BP were covalently linked to glutathione-Sepharose beads by using cross-linker dimethyl pimelimidate-HCl (80490, Sigma, St. Louis, MO). The crude serum was first subjected onto the GST column to remove the non-specific antibodies and the flow through were collected and loaded onto the GST-NS1-BP column. After washes, the antibodies were eluted by 0.1 M Glycine (pH 2.5) and immediately neutralized to pH 7.5 by 3M Tris-HCl (pH 8.8). The eluted fractions were collected and concentrated by a Centricon YM-30 (Millipore). The concentration of antibodies was adjusted

to 1 μg/μL and used for western blotting and immunostaining at a dilution of 1:1000 and 1:250, respectively.

hnRNP M monoclonal antibody (a gift from Dr. Maurice S. Swanson, University of Florida, FL) was used for western blot analysis at a 1:4000 dilution. hnRNP A1 monoclonal antibody (a gift from Dr. Michael Matunis, Johns Hopkins School of Public Health, MD) was used at a dilution 1:1000. NFAR polyclonal antibody (a gift from Dr. Glen Barber, University of Miami, FL) was used at a dilution 1:2000. hnRNP U monoclonal antibody (IQ210, ImmuQuest Ltd, North Yorkshire, UK) was used at a dilution 1:1000. E1B-AP5 polyclonal antibody (10578-1-AP, Proteintech Group Inc., Chicago, IL) was used at a dilution 1:2000. DHX9 monoclonal antibody (H00001660-M01, Abnova, Taipei, Taiwan) was used at a dilution 1:500. Polymerase II monoclonal antibody, clone CTD4H8 (05-623, Millipore, Temeculah, CA), was used at a dilution 1:5000. Influenza A PB1 polyclonal antibody (sc-17601, Santa Cruz Biotechnology, Inc., Santa Cruz, CA) was used at a dilution 1:5000. Antibodies specific to influenza A NS1 and M1/M2 proteins were gifts from Dr. Adolfo García-Sastre (Mount Sinai School of Medicine, NY). Anti-NS1 polyclonal antibody was used at a dilution 1:30,000, and anti-M1/M2 monoclonal antibody was used at a dilution 1:10,000. β-actin monoclonal antibody

(A1978, Sigma, St. Louis, MO) was used at a dilution 1:20,000. γ-tubulin monoclonal antibody (T5326, Sigma, St. Louis, MO) was used at a dilution 1:20,000.

2.5 RNA interference and Transfection

siRNA oligos (siGENOME SMARTpool) designed for silencing human IVNS1ABP gene were purchased from Dharmacon (D-016604-01, D-016604-02, D-016604-03, Thermo Fisher Scientific, Inc). Non-targeting siRNA, AUGAACGUGAAUUGCUCAAdTdT, synthesized by Dharmacon, together with siGENOME non-targeting siRNA #3 (D-001210-03) were used as controls.

The siRNAs were transfected with RNAiMAX reagent (Invitrogen) according to manufacture's instruction. A549 cells were seeded into 12-well plates at a density $1x10^5$ the day before transfection, and the cells were transfected with 50 nM of non-targeting siRNAs or siRNAs specific for NS1-BP. Knockdown efficiency was observed after 48-hour transfection by western blotting.

2.6 Immunoprecipitation and Mass Spectrometry

HeLa cells were washed and lysed with lysis buffer [50 mM Tris, pH 7.5, 150 mM NaCl, 1% IGEPAL CA-630 (I3021, Sigma), 0.1 mM Na_3VO_4, 1 mM NaF, 1mM DTT, 1mM EDTA, 1 mM PMSF, 1X complete protease inhibitor cocktail (04693132001, Roche), and 15% glycerol] for 20 min on ice. Cell lysates were centrifuged at 13,000xg for 15 min to pellet cellular debris. Supernatants were transferred into new tubes, and protein concentrations were determined by RC DC protein assay kit (500-0121, Biorad). 5 mg cell lysates were pre-cleared with protein A beads (17-0780-01, GE Healthcare) for 1 hour. The beads were discarded, and the pre-clear lysates were incubated with new protein A beads and 6 μg of control rabbit IgG (Santa Cruz Biotechnology, Inc.) or purified anti-NS1-BP antibody at 4°C for 2 hours. The beads were washes with lysis buffer four times, mixed with sample buffer, boiled for 5 min, and loaded onto a SDS-PAGE. After electrophoresis, the gel was stained with Colloidal blue (LC6025, Invitrogen). Each lane corresponding from 250 kDa to 30 kDa was excised into 8 segments, and gel pieces were subjected to in-gel digestions followed by LC/MS/MS analysis that were performed at the Protein Identification core facility at University of Texas Southwestern

Medical Center at Dallas. Electrospray mass spectrometry is performed on a ThermoFinnigan LTQ instrument, coupled with an Agilent 1100 Series HPLC system. The peptide mixtures were separated by a 75-micron i.d. reverse-phase C18 column. Acquired results were searched against the NCBI-nr protein database with Mascot software (Matrix Science).

2.7 SDS-PAGE and Western blot analysis

Gel electrophoresis was performed using the Tricine-SDS PAGE system as described elsewhere (Schagger and von Jagow, 1987). Acrylamide gels used in this study were 7%, acrylamide solution was 40%, and acrylamide/bis-acrylamide ratio was 5%. Running gel buffer was 1.5 M Tris-HCl, pH 8.45; stacking gel buffer contained 0.3 M Tris-HCl and 0.4% SDS, pH 7.8. Cathode buffer contained 0.1 M Tris, 0.1 M Tricine, and 0.1% SDS, pH 8.25. Anode buffer was 0.2 M Tris-HCl, pH 8.9. Thirty mL of the running gel mixture was prepared for 4 gels, which includes 5.25 mL of acrylamide solution, 10 mL of running gel buffer, 4 g glycerol, 10.64 mL water, 100 μL ammonium persulfate (10%), and 10 μL of TEMED (N,N,N',N'-tetramethylethane-1,2-diamine). The stacking gel mixture were 1.23 mL of acrylamide solution, 3 mL of stacking gel buffer, 7.77 mL of

water, 100 μL of ammonium persulfate (10%), and 10 μL of TEMED. Samples were mixed with equal volume of 2X sample buffer [100 mM Tris-HCl, 8% SDS, 24% glycerol, 200 mM DTT, and 0.02% bromophenol blue, pH 7.8], heated at 95°C for 10 min, and loaded onto the wells. The electrophoresis was performed at a constant voltage of 120 V until the tracking dye reached the edge of the gel.

After electrophoresis, proteins on the gel were transferred to a PVDF membrane (IPVH00010, Immobilon-P, Millipore) by using mini transfer electrophoretic cell (170-3930, Bio-Rad) with transfer buffer [20 mM Tris, 192 mM Glycine, and 10% methanol] at a constant voltage of 30 V overnight. The PVDF membrane was then blocked with 5% skim milk in PBS for 1 hour, followed by PBS-T (0.05% Tween 20 in PBS) wash twice, and incubated with primary antibody (prepared in 10 mg/mL BSA/PBS) at room temperature for 1 hour. After incubation, the membrane was washed 5 times with PBS-T buffer for 5 min each, and then incubated with HRP-conjugated secondary antibodies for another hour. Finally, the PVDF membrane was washed 4 times with PBS-T buffer for 10 min each, submerged in ECL reagent (34096, Pierce, Thermo Scientific) for 5 min, and exposed to a film in the dark room for 20 second to 5 min until the signal was visible.

2.8 Isolation of RNAs associated with NS1-BP

RNAs associated with NS1-BP were isolated as previously described (Conrad, 2008). A549 cells were grown in 10 cm dish to 90-100% (about $7.5x10^6$ cells) and infected with influenza virus (A/WSN/33) at MOI of 5 for 5 hours. Cells were washed with PBS and cross-linked with 0.3% formaldehyde (15710, Electron Mciroscopy Sciences, Hatfield, PA) in 10 mL PBS at room temperature for 10 min. Non-crosslink control was incubated with 10 mL PBS. Cross-link reaction was quenched by adding 1.25 mL of 2M glycine (pH 7.0) and incubated at room temperature for 5 min. Cells were harvested and lysed by cold RIPA-plus buffer [50 mM Tris (pH 8.0), 150 mM sodium chloride, 1% NP-40, 0.5% sodium deoxycholate, 0.1% SDS, 2 mM EDTA, 10 mM vanadyl-ribonucleoside complex (VRC; S1402S, New England Biolabs, Inc.), 1 mM PMSF, 1X protease inhibitor cocktail (Roche), and competitor RNA [2.5 mg/mL of torula yeast RNA (R6625, Sigma) and 0.5 mg/mL of polyuridylic acid potassium slat (poly-U; P9528, Sigma)]. Cell lysates were pass through a QiAshredder(Qiagen) twice and then centrifuged at 16,000 g for 10 min at 4°C. Twenty μL of lysates were saved as 5% input. Supernatant was pre-cleared with protein

A beads for 1 hour and then incubated with new protein A beads together with 6 μg of anti-NS1-BP antibodies or purified IgG from pre-immuned rabbit serum. Binding was allowed to proceed for 2 hours at 4°C. Twenty μL of lysates were saved as 5% supernatant. Beads were washed with 500 μL of cold RIPA buffer [50 mM Tris (pH 8.0), 150 mM sodium chloride, 1% NP-40, 0.5% sodium deoxycholate, 0.1% SDS, 2 mM EDTA], followed by 500 μL of RIPA-U-plus buffer (RIPA buffer supplemented with 1M urea and competitor RNA) for 10 min twice, 500 μL of RIPA-U buffer (RIPA buffer supplemented with 1M urea) twice, and with 500 μL of cold RIPA buffer. The 100% beads, the 5% of input, and 5% of supernatant were mixed with 130 μL of reverse buffer [10 mM Tris (pH 6.8), 5 mM EDTA, 10 mM DTT, and 1% SDS] and followed by incubation at 70°C for 45 min to reverse the cross-link. Samples were then mixed with 150 μL of 2x Proteinase K solution [40 mM Tris (pH 7.5), 5 mM EDTA, 45 ng/μL of GlycoBlue (AM9515, Ambion), 0.2 mg/mL of torula yeast RNA] and incubated at 37°C for 30 min. 30 μL of 3M sodium acetate (pH 5.2) and 350 μL of Phenol:Chloroform:Isoamyl Alcohol (25:24:1 PCA, 15593-031, Invitrogen) were added into the tubes, mixed, and centrifuged at 16,000xg for 5 min at room temperature. The supernatant was transferred into a tube containing 900 μL of 100% ethanol and stored at -20°C overnight.

The RNA was pelleted by centrifugation at 16,000xg for 15 min at room temperature, and the pellet was washed with 70% ethanol and dried at room temperature. Next, the pellet was resuspended in 20 μL of RNase-free water, mixed with 20 μL of 2x DNase I solution [2 U/μL of RNase inhibitor (3335402, Roche), 2x DNase buffer, 0.2 U/μL DNase I (04716728001, Roche)], and incubated at 37°C for 45 min. Then 180 μL of G-50 buffer [0.25% SDS, 20 mM Tris (pH 7.0), 0.3 M sodium acetate, and 2 mM EDTA] and 200 μL of PCA were added to the tubes, and RNA were pelleted and washed as described.

RNAs were reversed transcribed into cDNA and analyzed by qPCR; primers used in reverse transcription and PCR were described in section 2.9 and table1. The amount of RNA was calculated as 2^{-Ct}, and the pull-down RNA was normalized to input amount and calculated as the percentage of IP [$\%IP=(2^{-Ct\ IP}/2^{-Ct\ input}) \times 5\%$]. To show the relative amount of different viral RNA segments, I set the %IP of pull-down M segment as one, and the %IP of each segment was further normalized to the M segment. The final data were displayed as relative RNA level.

2.9 RNA purification and RT-qPCR

Total RNAs were isolated from A549 cells by High Pure RNA Isolation Kit (11828665001, Roche). 0.5 μg of total RNAs were reverse transcribed into cDNA by SuperScript II reverse transcriptase (18064014, Invitrogen); reactions were set up according to the manufacturer's protocol in the presence of 1 μM of specific primers as follows. Uni12 primer (5'-AGCAAAAGCAGC-3') was used for vRNA (Hoffmann et al., 2001), oligo-$(dT)_{15}$ for mRNA, cRNA primer (5'-ATATCGTCT CGTATTAGTAGAAACAAGG-3') for viral cRNA (Ge et al., 2003), and reverse primer of RPL32 (5'-ACTCATTTTCTTCGCTGCGT-3') for host ribosomal protein L32. RT was carried on 42°C for 1hour and inactivated by heating at 80°C for 20 min.

Then the RT reactions were diluted with water at a ratio 1:5, and 1.25 μL of cDNA mixture was subjected to quantitative real-time PCR (qPCR) using SYBR green I Master (04707516001, Roche) combined LightCycler 480 System (Roche). qPCR was carried out by initial denaturation at 95°C for 3 min, 40 cycles of 95°C for 15 sec, 60°C for 15 sec, 72°C for 20 sec, and followed by a melting curve cycle from 65°C to 95°C for quality assurance. All reactions were done in duplicates. Gene-specific primers

were designed by D-LUX^{TM} program (Invitrogen) and validated by analysis of template titration and dissociation curves. All primers had efficiencies between 90-100%. Primer sequences were listed in table1. qPCR results were evaluated by comparative Ct method ($\Delta\Delta$Ct) using RPL32 gene as the invariably internal control. The data was presented as the relative viral RNA ratio of NS1-BP siRNA to non-targeting siRNA control.

2.10 Luciferase assay for influenza RdRp activity

Influenza mini-genome reporter construct (vPol-Luc) was induced by the viral polymerase complex through infection or transfection of viral polymerase constructs (NP, PB1, PB2, and PA) at an optimized ratio of 2:1:1:1. For the assay in which luciferase was induced by infection, A549 cells were seeded into 24-well plates at a density of $7.5x10^4$ cells/well the day prior to siRNA transfection. Each well was treated with 50 nM non-targeting siRNA or NS1-BP siRNAs together with 0.2 μg of vPol-Luc construct. After 48-hour transfection, cells were infected with virus at an MOI of 2.5, and infections were allowed to proceed for 16 hours. Cells in each well were then lysed with 125 μL of reporter lysis buffer (E4030, Promega, Madision, WI) and mixed on a shaker at room temperature for

20 min. Fifteen μL of lysates from each well were transferred in duplicate into two 96-well white plates (3903, Corning). Thirty μL of Luciferase substrate (E1500, Promega) was added into each well of the first 96-well plate, and 50 μL of CellTiter-Glo reagents (G7572, Promega) were added into each well of the second plate. Luminescence was measured with the EnVision multimode plate reader (PerkinElmer Inc., Waltham, MA).

For assays in which luciferase was induced by transfection of plasmids encoding the viral polymerase complex, the protocol was similar as described above except for some minor modifications. The cell density was $5x10^4$ cells/well, and after 48-hour knockdown, a second transfection was done using Lipofectamine 2000 (Invitrogen) containing 0.2 μg of vPol-Luc, 62.5 ng of pcDNA-NP, and 31.25 ng of each pcDNA-PB1, pcDNA-PB2, and pcDNA-PA construct. The transfection was allowed to proceed for 16 hours. Then cells were lysed, and luminescence was measured as described above. For data analysis, in each well, the luciferase signal was normalized to its CellTiter-Glo signal to eliminate the effect due to cell death. Then the results were presented as relative luciferase activity to the non-targeting siRNA control. Mock infection and transfections of PB1-deficient polymerase complex were used as negative-controls to ensure

that the luciferase signals were only driven by functional viral polymerase complex.

2.11 Click-it captures nascent RNA experiment

To monitor the synthesis of viral RNAs, I labeled the nascent virus RNAs using an assay (C10365, Invitrogen), in which 5-ethynyl uridines (EU), an analog of uridine, was incorporated into newly synthesized RNAs. The experiment was performed according to manufacture's protocol. In brief, A549 cells, in 24-well plates, were transfected with non-targeting or NS1-BP siRNAs as described in the previous section, and knockdown was allowed to proceed for 48 hours. Cells were infected with influenza virus at MOI 2. After 45 min adsorption, cells were washed with PBS three times and then overlaid with infection media including 0.5 mM of EU. At each time point, total RNA was isolated, and 2 μg of RNA were subjected to a copper-catalyzed reaction with azide-modified biotin in a 50 μL reaction. RNAs were further precipitated with 700 μL of 100% ethanol containing 0.05 μg/μL glycogen and 0.5 M ammonium acetate. To purify EU-RNA, 500 ng of RNA was incubated with 8 μL of streptavidin beads in a 40 μL reaction mix at room temperature for 30 min. After final wash, the beads

were resuspended in 10 μL RNase-free water and then mixed with 15 μL of reverse transcriptase mix [5 μL of 5x RT buffer, 2.5 μL of 0.1 M DTT, 1 μL of dNTP mix (10 mM each), 2 μL of oligo-dT (10 μM) or viral specific primers (10 μM), 0.5 μL of RNase inhibitor (40 U/μL), 3 μL of water, and 1μL of SuperScript II reverse transcriptase]. The reactions were carried on a thermomixer at 42°C for 80 min with gently mixing (1000 rpm) to avoid beads precipitation and then heated at 80°C for 20 min to terminate the reactions. Tubes were placed on a magnetic stand, and the supernatants were transferred and diluted with water at a ratio of 1:4. The RT mix 1.25 μL was analyzed by qPCR. Control experiments were performed as described above except that there was no EU in the media. This control was used to correct the background binding to the magnetic beads. The Ct number of each time point was converted to 2^{-Ct}, then the control signal was subtracted from the experimental data set ($2^{-Ct\ exp}$-$2^{-Ct\ no\ EU}$), and data were presented as relative amount to non-targeting siRNA.

2.12 Expression and Purification of GST-NS1-BP

Plasmid pGEX-NS1BP was transformed into bacteria strain BL21(DE3). A single colony was inoculated into 2.5 mL of LB with 100

μg/mL of ampicillin and incubated at 37°C in a shaker at 225 rpm overnight. Next day, the overnight culture was added into 250 mL of 2-YT broth (22712020, Invitrogen) and grown to OD 0.6 at 37°C. Protein expression was induced by 0.2 mM isopropyl-beta-D-thiogalactopyranoside (IPTG) at 20°C for 6 hours. Bacteria were pelleted and resuspended in 25 mL of cold lysis buffer [20 mM HEPES, pH 7.5, 1 mM EDTA, 300 mM NaCl, and 1x protease inhibitor cocktail (Roche)]. Cells were lysed by five passages through an EmulsiFlex-C5 homogenizer (Avestin, Canada) at 8000 psi, and lysates were centrifuged at 13,000xg for 15 min. The supernatant was incubated with 2 mL (50% slurry) glutathione Sepharose beads at 4°C for 1 hour, and beads were washed 10 times with cold lysis buffer. Washed beads were mixed with 1mL of 2x sample buffer and subjected to a SDS-PAGE. After electrophoresis, the protein band was located by staining the side strip of the gel with Coomassie blue solution [0.02% Coomassie Brilliant Blue G-250, 10% ethanol, and 2% orthophosphoric acid (85%)]. Protein band was excised, washed twice with PBS for 30 min, and used as antigen to raise polyclonal antibodies.

2.13 In vivo splicing assay

Minigene CD1 and CD9 constructs were derived from gene CD45, a receptor-like tyrosine phosphatase that regulates T cell-mediated signal transduction. These constructs were previously described (Rothrock et al., 2003). CD45 gene includes three variable exons (4, 5, and 6); alternative splicing of these exons results in five different isoforms (Zikherman and Weiss, 2008). CD1 minigene contains the variable exon 4 that is more susceptible to alternative splicing and flanked by two constitutive exons, termed 3 and 7. In contrast, CD9 minigene includes a constitutive exon 9 that is more resistant to alternative splicing. Minigene constructs encoding transcripts with variable splicing ability were used as substrates to test whether knockdown of NS1-BP has a role in the regulation of splicing. HeLa cells were seeded in 6-well plate at a density of $2.5x10^5$ per well the day before transfection. At the 2^{nd} day, cells were co-transfected with 50 nM of non-targeting or NS1-BP siRNAs together with 0.5 μg of CD1 or CD9 plasmid using Effectene as transfection reagent (301425, Qiagen, CA). After 72 hours of transfection, one tenth mL of cells were lysed by sample buffer for western blot, and the remaining cells were harvested for

RNA purification using RNA-Bee (Tel-Test, Friendswood, TX) according to manufacture's instruction. For analysis of the splicing products, a low-cycle RT-PCR protocol was performed (Lynch and Weiss, 2000). In brief, 1 μg of RNA was heated at 90°C and allowed to cool down gradually to 43°C in the presence of 1 ng of reverse primer (5'-GCGAGCTTCAGTGATACTTGTGGGCC-3'), 375 mM NaCl, 12.5 mM Tris (pH 7.5), and 2.5 mM EDTA. The annealed reaction was then diluted with a RT mixture to final concentrations of 10 mM Tris (pH 7.5), 6 mM $MgCl_2$, 1 mM dNTPs, 10 mM DTT, 62.5 mM NaCl, and 0.5 μL M-MLV reverse transcriptase (Promega). The reaction was incubated at 43°C for 30 min and terminated by boiling for 5 min.

PCR was performed as following: 5 μL of the RT reaction was diluted with a PCR mix to final concentrations of 7.5 mM Tris (pH 7.5), 37.5 mM KCl, 1.125 mM $MgCl_2$, 0.25 mM dNTPs, 5 ng of forward primer (5'-GGTTCGGCTTCTGGCGTGTGACCG-3'), 2.5 ng of reverse primer (5'-GCGAGCTTCAGTGATACTTGTGGGCC-3'), 2.5 ng of ^{32}P-labeled reverse primer, and 1 unit of Taq polymerase. PCR sample were denatured at 94°C for 2 min, followed by limiting cycles of 94°C for 1min, 70°C for 1 min, and 72°C for 1.5 min. The PCR products were resolved in a 5% denature polyacrylamide gel. After electrophoresis, gel was fixed (10%

methanol and 10% acetic acid) for 15 min, dried at 80°C for 1 hour, exposed to a PhosphoImager plate for 3 hours, and quantified by a Typhoon Imager (GE Healthcare).

2.14 Immunostaining and Fluorescence Microscopy

A549 cells were seeded in 12-well plates at a density of $1x10^5$ cells/well the day before siRNA transfection. At the second day, cells were treated with 50 nM of non-targeting or NS1-BP siRNAs. After 24 hours, cells in each well were trypsinized and split into 4 wells of 24-well plate including a coverslip per well, and incubated for another 24 hours. To synchronize the infection, cells were pre-chilled on ice for 10 min before infection, washed by cold PBS, and infected with virus at MOI 10. After 45 min adsorption on ice, cells were washed by PBS and overlaid with 0.5 mL of warm infection media. At each indicated time point, cells on coverslips were fixed by 3% formaldehyde/PBS at room temperature for 15 min, washed with PBS three times, and then permeabilized with 0.5% TritonX-100/PBS at room temperature for 5 min. Then coverslips were incubated with NP antibody prepared in BSA solution (1 mg/mL) at a dilution of 1:3200 at room temperature for 1 hour. After washed in PBS three times, the coverslips

were incubated with Alexa Fluor 488 donkey anti-mouse IgG (A-11001, Invitrogen) at a dilution of 1:500 in BSA for another 1hour, followed by PBS wash three times. The coverslips were further incubated with Hoechst (0.5 μg/mL) (H-1399, Invitrogen) at room temperature for 5 min and washed in PBS. After the final PBS wash, coverslips were mounted onto glass microscope slides with mounting media (S-3023, Dako, Denmark). Images were taken and processed by using Zeiss Axioplan 2E microscope, Hamamatsu monochrome digital camera, and OpenLab software.

CHAPTER THREE

RESULTS

3.1 Characterized the co-precipitated proteins of myc-NS1BP and raised antibodies against endogenous NS1-BP

To study the functions of NS1-BP, I first investigated its binding partners. Using HeLa cells transfected with myc-NS1BP, I performed immunoprecipitation studies with anti-myc antibodies (Figure 5A). A protein of 95 kD bound specificially to NS1-BP was identified by mass spectrometry as valosin-containing protein (VCP), which is an ATPase that functions as a chaperone in the ubiquitin-proteasome degradation pathway (Wang et al., 2004). To further examine the specificity, I expressed other myc-tagged proteins, hnRNPA1 and WBS (Williams-Beuren syndrome chromosomal region 16 protein), and performed immunoprecipitation in the same conditions. I found that VCP was co-precipitated with myc-hnRNPA1 and WBS (data not shown), suggesting that VCP may be a non-specific protein randomly pulled down by anti-myc antibodies. Since protein overexpression can cause mislocalization, which may allow proteins to interact with binding partners that they did not

normally have access in the cell, I decided to investigate the interacting partners of endogenous NS1-BP.

Using the GST-NS1BP full-length protein as an antigen, I raised polyclonal antibodies that were able to recognize endogenous NS1-BP at the predicated size of 70 kDa and three other minor bands (60 kDs, 45 kDa, and 35 kDa), which may be derived from the degraded NS1-BP or the cross-reacted cellular proteins (Figure 5B). The specificity of antibody was verified by siRNA oligos targeted to NS1-BP (Figure 5C). Moreover, immunostaining showed that most NS1-BP localized in the nucleus, whereas there were a small subset of NS1-BP localized in the cytoplasm (Figure 5D). The recognition pattern of NS1-BP antibodies was consistent with a previous study (Wolff et al., 1998), confirming the successful development of NS1-BP antibody.

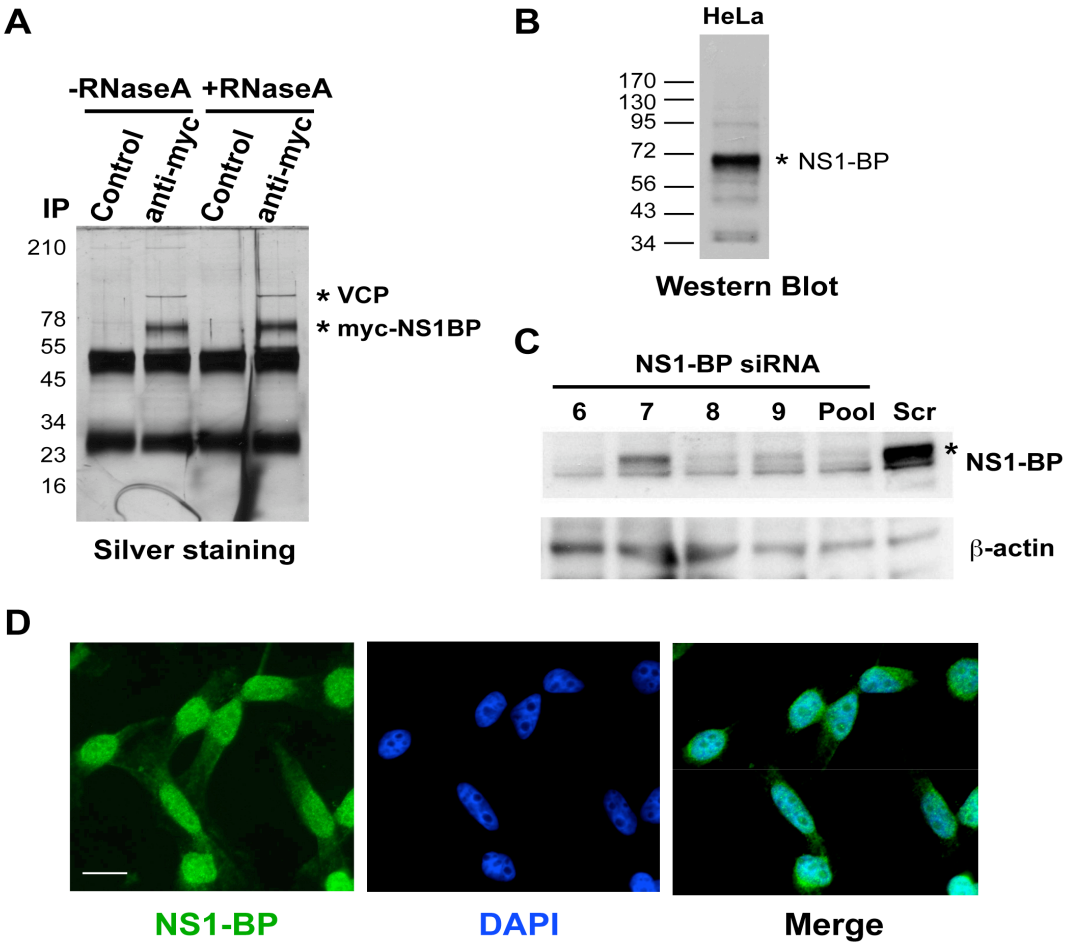

Figure 5. Characterized the co-precipitated proteins of myc-NS1BP and raised antibodies against endogenous NS1-BP. (A) HeLa cells were transfected with plasmid encoding myc-NS1-BP, and lysates were immunoprecipitated with control IgG or anti-myc antibodies. The binding proteins were resolved in SDS-PAGE and identified by mass spectrometry (asterisk). (B) Twenty microgram of HeLa cell lysates were subjected to SDS-PAGE. Proteins were transferred to PVDF membrane and probed with affinity-purified NS1-BP antibodies. (C) HeLa cells were transfected with non-targeting or NS1-BP siRNAs for 48 h, and 20 μg of lysates were subjected to immunoblot analysis as in (B). Membrane was probed with anti-NS1-BP and β-actin antibodies. The latter was used as a loading control. (D) HeLa cells were grown on coverslips and subjected to

immunofluorescence microscopy with affinity-purified NS1-BP antibodies (green) and DAPI stining (blue). Scale bar: 10 μm.

3.2 Endogenous NS1-BP interacts with RNA-binding proteins

I then performed immunoprecipitation with affinity-purified NS1-BP antibodies and identified the interacting proteins from 250 kDa to 35 kDa by mass spectrometry. Interestingly, the results showed a complete different binding pattern compared to myc-NS1-BP immunoprecipitation (Figure 6A). Among these associated proteins, enolase1 and β-actin have been previously shown to directly interact with NS1-BP (Perconti et al., 2007; Sasagawa et al., 2002), which served as positive controls for our immunoprecipitation. Most interacting partners were RNA-binding proteins and can be classified into different categories including heterogeneous nuclear ribonucleoprotein (hnRNP family), RNA helicase (DEAD box polypeptide family), antiviral proteins (nuclear factor associated with dsRNA (NFAR-2), zinc finger antiviral protein), poly(A) binding protein, and nuclear cap binding protein, chaperone molecule (Hsp70 and Hsp90), and DNA damage repaired protein (poly (ADP-ribose) polymerase, PARP) (Figure 6B, table 2). I next examined whether these interactions were RNA-dependent or independent. I performed the same

immunoprecipitation in the absence or presence of RNaseA and used antibodies to verify the binding specificity. In the absence of RNaseA, NS1-BP indeed interacted with those RNA-binding proteins identified by mass spectrometry (Figure 7A, lane 3 and 4). However, in the presence of RNaseA, most interactions were lost, except hnRNP M, which showed a slight decrease in binding to NS1-BP (Figure 7A, lane 5 and 6).

Although NS1-BP does not have a consensus RNA recognition motif (RRM), these results suggested that it might be an RNA-binding protein and engaged in the process of gene expression and mRNA processing, directly or indirectly. To investigate the functions of NS1-BP, I reviewed the literature and looked for the signaling signatures that connected to our results of mass spectrometry. Interestingly, two proteomic analyses identify similar proteins (PARP-1, NFAR-2, poly(A)-binding proein C, hnRNPM, hnRNPA1, DDX17, Hsp70, and Hsp90) interacting with influenza A viral ribonucleoprotein (vRNP) or the heterotrimeric polymerase complex (Jorba et al., 2008; Mayer et al., 2007). In addition, this host-influenza polymerase interactome also identified the largest subunit of human RNA polymerase II (Pol II CTD), which has been known to bind viral polymerase complex (Engelhardt and Fodor, 2006; Engelhardt et al., 2005). Since NS1-BP shared similar binding proteins to the host-

influenza polymerase interactome, I reasoned that NS1-BP might interact with cellular RNA polymerase II and viral polymerase complex to mediate viral polymerase activity.

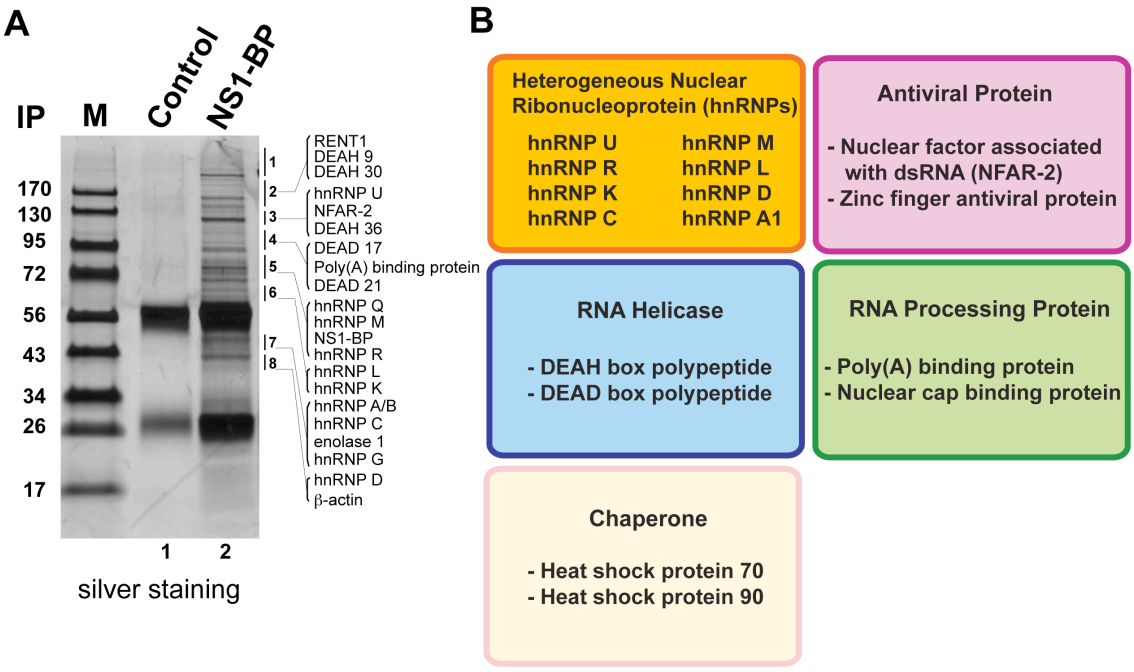

Figure 6. NS1-BP interactes with RNA-binding proteins. (A) HeLa cell lysates were immunoprecipitated with control IgG or antibodies specific for NS1-BP in the absence of RNase A. Interacting proteins were resolved by SDS-PAGE and identified by mass-spectrometry. The lane was divided into eight segments from molecular weight 250 kDa to 35 kDa, and the top hits in each segment were listed in the parentheses. (B) The interacting partners of NS1-BP were classified into five major categories as indicated.

3.3 NS1-BP interacts with cellular RNA polymerase II and influenza virus polymerase complex

If NS1-BP interacts with cellular RNA polymerase II (Pol II CTD), this supports our hypothesis that NS1-BP may play a role in gene transcription. Though I did not identify cellular Pol II CTD by mass spectrometry, I still have to consider the possibility of the limited detection of mass spectrometry; especially because Pol II CTD is a hyperphosphorylated protein, the hydrophilic property of phosphopeptides can interfere with the binding to the hydrophobic C18 column, which may cause a significant loss in peptide recovery. To examine whether NS1-BP interacted with Pol II CTD, I immunoprecipitated NS1-BP and probed the precipitated proteins with antibody against total Pol II CTD. Indeed, NS1-BP interacted with Pol II CTD; moreover, this interaction was RNA-independent (Figure 7B). I next tested whether NS1-BP associated with the viral polymerase complex. Immunoprecipitation was performed using A549 cell lysates from cells with or without virus infection, and the results showed that NS1-BP bound to the influenza viral polymerase (Figure 7C).

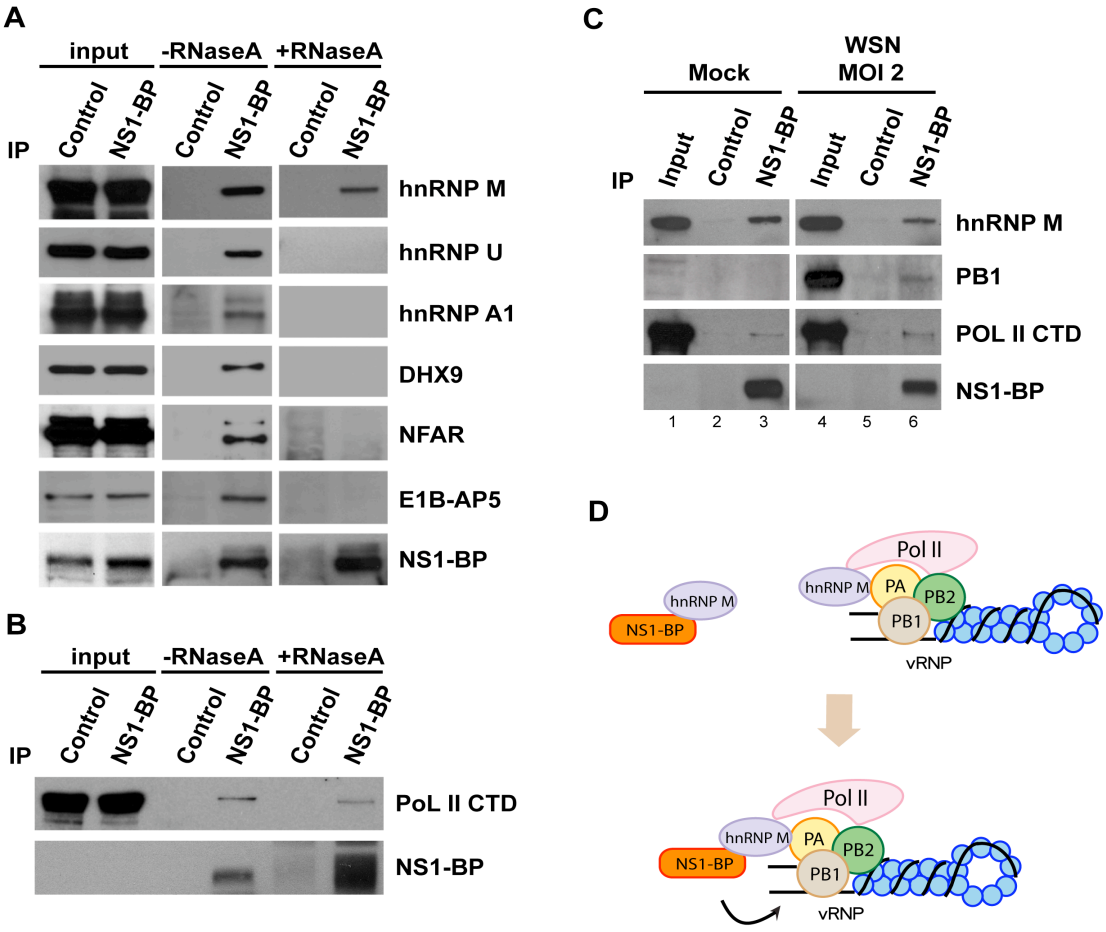

Figure 7. NS1-BP forms a complex with the cellular RNA polymerase II and influenza virus polymerase. (A) RNase A disrupts the interaction of NS1-BP with RNA-binding proteins. HeLa cell lysates were immunoprecipitated with control IgG or antibodies against NS1-BP in the absence or presence of 1 μg/mL RNase A. The PVDF membrane was probed with several antibodies as indicated, and 2% of lysates were loaded as input. (B) Interaction of NS1-BP and host RNA polymerase II CTD (Pol II CTD) was RNA-independent. Immunoprecipitation was performed as described in (A), and 0.5% of lysates were loaded as input. (C) A549 cells were non-infected or infected with influenza virus (A/WSN/33) at MOI 2 for 16 h. Cell lysates were immunoprecipitated with control IgG or anti-NS1-BP antibodies, and 0.5% of lysates were loaded as input. Membrane was probed with the indicated antibodies. (D) The

model shows that NS1-BP interacts with cellular polymerase II and viral RNA polymerase via hnRNP M.

3.4 Low levels of NS1-BP decrease viral polymerase activity

Since NS1-BP interacted with viral polymerase, I next examined whether NS1-BP regulated viral polymerase activity. To test this idea, I employed a viral mini-genome system that has been used in previous studies to monitor viral polymerase activity (Hoffmann et al., 2008). In this system, the plasmid is driven by cellular RNA polymerase I first and expresses a negative-sense luciferase RNA with influenza cRNA promoter. Then this RNA transcript, mimicking the viral RNA, is further transcribed into mRNA by influenza polymerase complex. Finally, the luciferase mRNA is translated and detected in the cytoplasm. This system is induced by either virus infection or transfection with viral polymerase constructs (Figure 8A).

I co-transfected A549 cells with the plasmid encoding mini-genome reporter and non-targeting or NS1-BP siRNAs and infected the cells with influenza virus (A/WSN/33) at 48 h post-transfection. Compared to non-targeting siRNA, NS1-BP knockdown showed a significant decrease in luciferase activity about 3.7 to 17 fold using different NS1-BP siRNAs (p value < 0.05) (Figure 8B, right). In contrast, I did not detect any luciferase

signal in mock infection control, indicating that the signal is only driven by the viral polymerase (Figure 8B, left).

As influenza NS1 protein has been known to target cellular NS1-BP, I next examined whether the decrease of viral polymerase activity in NS1-BP siRNA-depleted cells was due to NS1 activity. Instead of infecting cells, I transfected cells with plasmids encoding the mini-genome reporter and the viral polymerase complex after 48 h of siRNA depletion. In this manner, I eliminated a potential effect of NS1 and of other viral proteins on viral polymerase activity. Consistent with the result obtained by infection, viral polymerase activity in this transfection assay also decreased in NS1-BP depleted cells about 3 to 9 fold using different siRNAs. In contrast, there was no signal detected in control, in which cells were transfected with other components of the polymerase complex except PB1 (Figure 8D).

To rule out the possibility that the decrease of viral polymerase activity in NS1-BP depleted cells was due to the cell death induced by siRNA transfection or viral infection, I examined cell viability by measuring the amount of cellular metabolic ATP, which is in proportional to viable cell number. Compared to non-targeting siRNA, NS1-BP siRNA-depletion showed a slight reduction in cell number from ratio 1 to 0.75-0.9 among

different siRNA oligos in infection assay (Figure 8C). For transfection assay, compared to non-targeting siRNA, cells deaths slightly increased; ratio dropped from 1 to 0.54-0.7 among different siRNA oligos, which may be due to the cytotoxicity of double transfections (Figure 8E). Considering the effect of cell death, I normalized luciferase activity to the cell viability (Figure 8B and 8D). Indeed, NS1-BP knockdown reduced viral polymerase activity.

To further rule out the possibility that NS1-BP knockdown affected the cellular RNA polymerase I, which was responsible for transcribing the negative-sensed luciferase RNA, I examined the activity of RNA polymerase I by measuring one of its products, 18S rRNA. Compared to non-targeting siRNA, NS1-BP knockdown did not cause significant change in 18S rRNA level, indicating the reduction of viral polymerase activity was not due to the decreased expression of negative-sensed luciferase transcripts (Figure 8F).

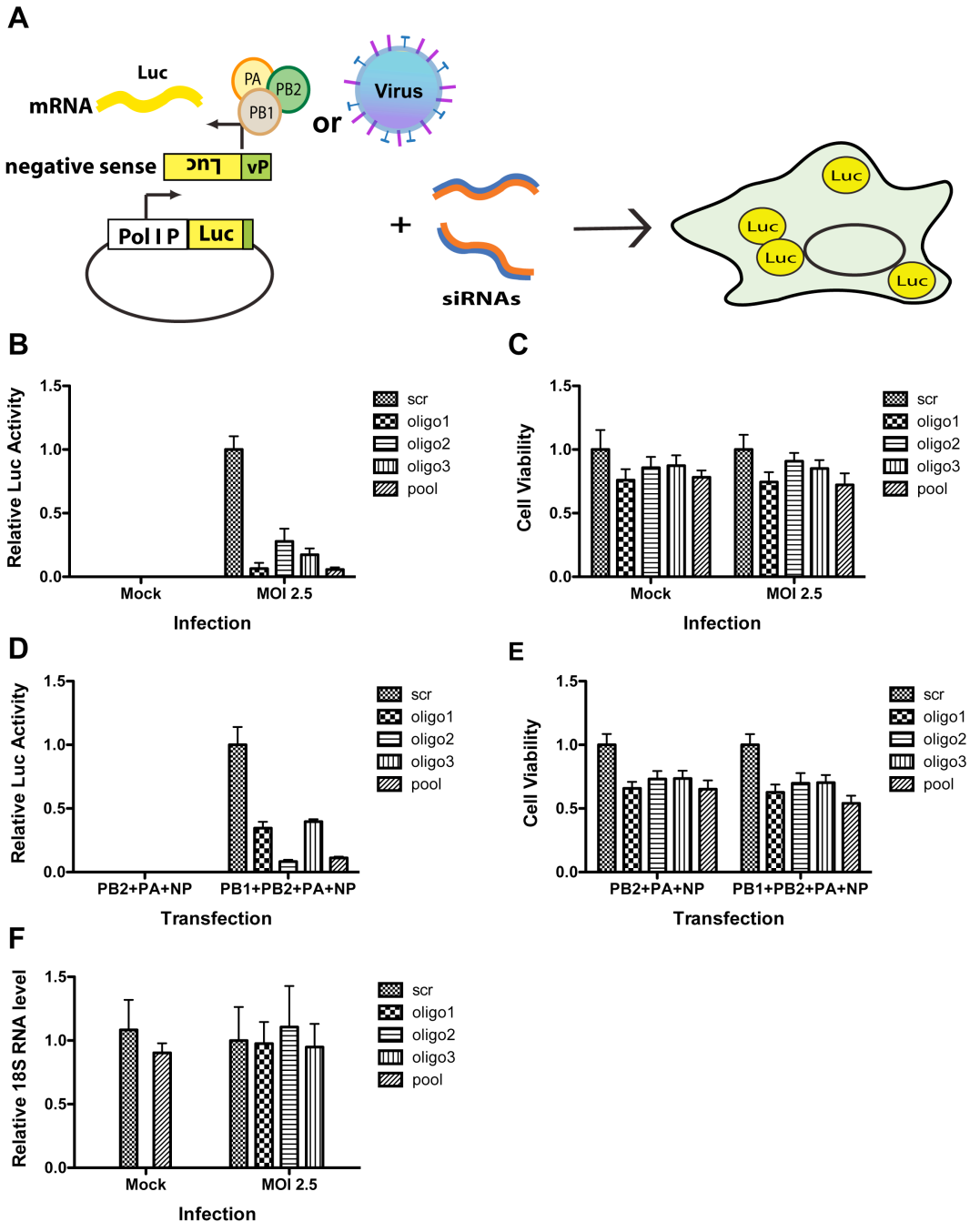

Figure 8. Low levels of NS1-BP decrease viral polymerase activity. (A) The schematic explains gene expression driven by the influenza mini-genome reporter system. (B) A549 cells were co-transfected with the viral polymerase mini-genome reporter construct and non-targeting or NS1-BP

siRNAs for 48 h and then infected with influenza virus at MOI 2.5 for 16 h. The luciferase avtivity was normalized to cell viability and presented as relative viral polymerase activity to non-targeting siRNA control. (C) The duplicated lysates from figure B were used as a control of cell death. The cell viability was measured using CellTiter-Glo; the luminescence signal was normalized to non-targeting siRNA control and displayed as a relative level. (D) After 48 h knockdown, instead of infection, cells were transfected with constructs of the mini-genome reporter and viral polymerase complex (PB1, PB2, PA, and NP) (E) The duplicated lysates from figure D were used as a control of cell death. The cell viability was measured by CellTiter-Glo; the luminescence signal was normalized to non-targeting siRNA control and displayed as a relative level. (F) A549 cells in parallel 24-well plates were treated with same conditions as the cells in (B), but the cells were harvested for RNA purification. Random hexamer was used in the reverse transcription reaction, and the qPCR results were presented as relative to non-targeting siRNA in both mock and cells infected at MOI 2.5. Mock infection and transfection of PB1-deficinet viral polymerase complex were used as controls in figure B and D, respectively, to ensure that the Luc signal was only derived from a functional polymerase complex. Error bars mean standard deviation from three independent experiments (p value < 0.05).

3.5 NS1-BP depletion decrease viral replication and viral protein expression

I showed that low levels of NS1-BP decreased viral polymerase activity, I next examined whether the progression of viral life cycle was altered. I transfected A549 cells with non-targeting or NS1-BP siRNA for 48 h and infected the cells with influenza virus at MOI 0.001. After 24 h and 36 h post infection, supernatants were collected, and virus titer was determined using plaque assay. Knockdown efficiency of siRNAs was evaluated by

western blot analysis at 48 h post-transfection (Figure 9E). Compared to the control, NS1-BP depleted cells showed a significant decrease in virus replication. At 24 h post infection, as compared to the control, the fold change of viral titer decreased 3.6 to 22 fold among different siRNA oligos; at 36 h post infection, the fold change decreased 3.3 to 12 fold among different oligos (Figure 9A and 9B). Cell viability was measured at each time point as indicated, and the results did not show significant difference between control and siRNA depletion or virus infection, suggesting that the decrease of virus replication in NS1-BP depleted cells was not due to cell deaths (Figure 9C and 9D).

I next investigated the mechanism involved in the decrease of viral replication by examining the viral protein expression under NS1-BP depletion. Viral protein expression showed an obvious reduction at 6 h to 7 h post-infection (Figure 9F, lane 5 and lane 6), and the effect was gradually diminished at later time points. M2 protein is expressed at late stages of the viral life cycle (Odagiri et al., 1999). As expected, I observed reduced protein expression of M2 after 8 h post-infection (Figure 9F, second row).

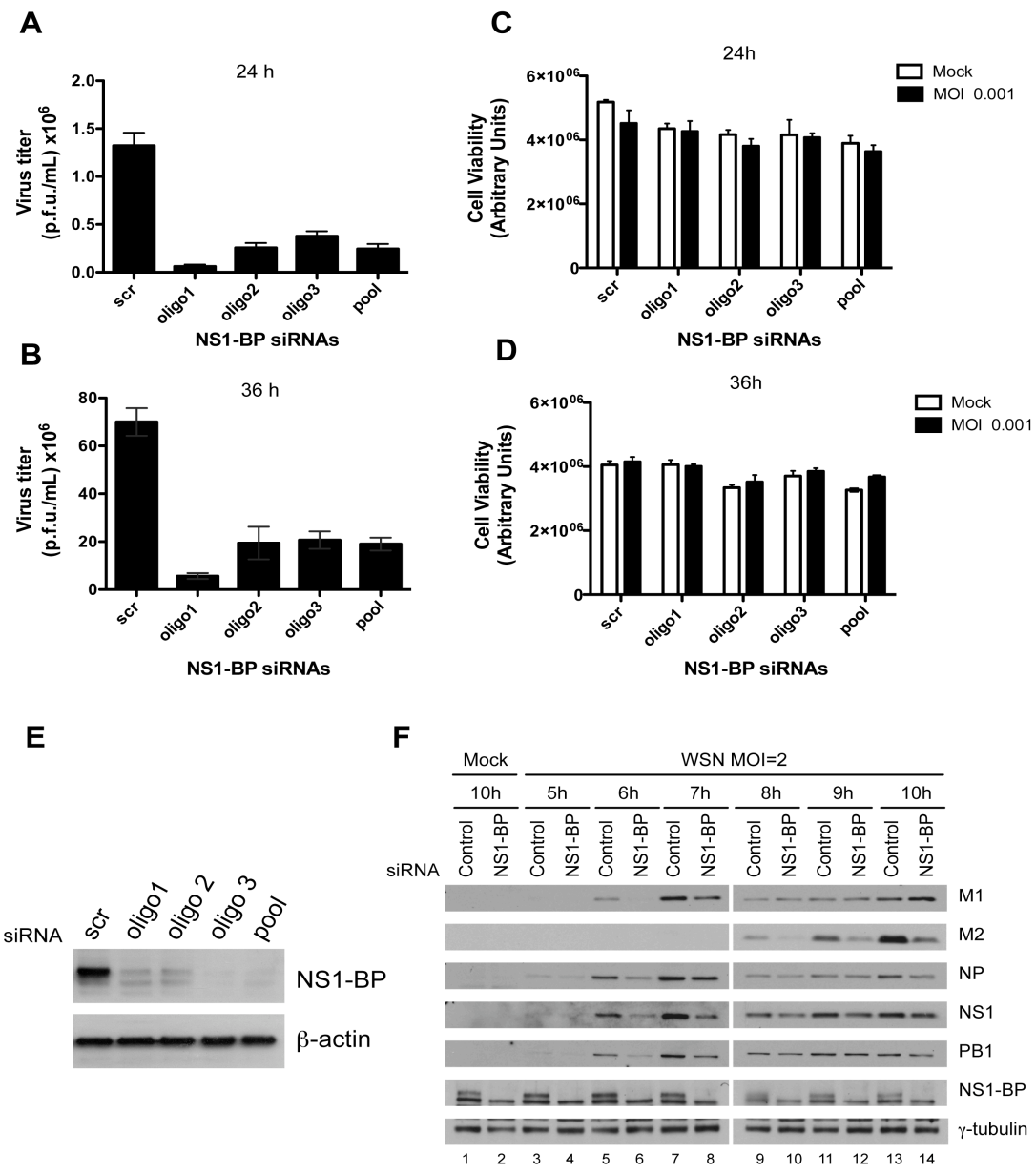

Figure 9. Low levels of NS1-BP decrease influenza replication and viral protein expression. A549 cells were transfected with non-targeting or NS1-BP siRNAs for 48 h. (A) and (B) The cells were infected with virus at MOI 0.001. The supernatants were harvested at 24 h and 36 h post-infection, and virus titer was determined by plaque assay. Mock infection

did not show any plaque (data not shown). (C) and (D) After the removal of the supernatant, the remaining cells were lysed, and cell viabilitiy was measured by CellTiter-Glo at 24 h and 36 h post-infection. This data shows that low level of NS1-BP decrease virus replication, which is not due to cell death. (E) The knockdown efficiency was verified by western blot analysis. (F) A549 cells were transfected with non-targeting or NS1-BP siRNAs for 48 h and infected with influenza virus at MOI 2 for the indicated time points. Cells were lysed with sample buffer, and 5 μg of lysates were resolved by SDS-PAGE. The membrane was probed with antibodies against several influenza virus proteins. Gamma-tubulin was used as a loading control.

3.6 NS1-BP regulates virus RNA synthesis

Since NS1-BP depletion down regulated viral protein expression, I asked whether this effect resulted from low levels of viral mRNAs or from unstable viral proteins. First, using real-time RT-PCR, I compared the amount of influenza virion RNA (vRNA), complementary RNA (cRNA), and viral mRNA in control and NS1-BP depleted cells. I used siRNAs to deplete NS1-BP for 48 h and infected the cells with virus at MOI 2 for 1 to 5 hours. The relative amount of viral RNAs was presented as a ratio of NS1-BP siRNA-depletion to the control. I measured PB1, PA, NS, M, and NP segments in three types of viral RNAs. The RNA level of cellular RPL32 is relatively more constant than general housekeeping gene (e.g. GAPDH and β-actin; data not shown) upon influenza virus infection; therefore I chose RPL32 as an internal control (Figure 10F). The

knockdown efficiency of NS1-BP was about 70% to 80% (Figure 10G). I included mock infection in every qPCR experiment as a control and did not detect any signal, suggesting that the primers used in the qPCR reactions are highly specific to the viral genome without cross-reactions with cellular RNAs.

The ratio of viral mRNA fluctuated between 1 h to 3 h post infection. It decreased at beginning, then slightly increased, but then showed an obvious reduction at 3 h post infection in all segments I examined (Figure 10 A-E). After 3 h post-infection, the viral mRNA levels gradually rose, and this effect might be due to the recovery of NS1-BP protein levels as virus infection might block the siRNA function. The cRNA, which serves as a template for vRNA replication, was significantly decreased in all segments at 3 h post infection though the level slightly rose later in the case of M and NS segment (Figure 10 J&K). Interestingly, the cRNA of polymerase PB1 and PA showed a pronounced progressive decrease upon infection (Figure 10 H&I). Since cRNA levels decreased in NS1-BP depleted cells, as expected, I also observed a reduction of the virion RNAs (vRNA), especially in the viral polymerase segments, PB1 and PA. (Figure 10 N&O). In conclusion, NS1-BP depletion reduced the production of three types of viral RNAs. Among these, viral mRNA showed an earlier effect

than the other two types, which is consistent with the model that influenza virus starts its life cycle with transcription (viral mRNA) and then switches to replication (cRNA and vRNA) (Hay et al., 1977).

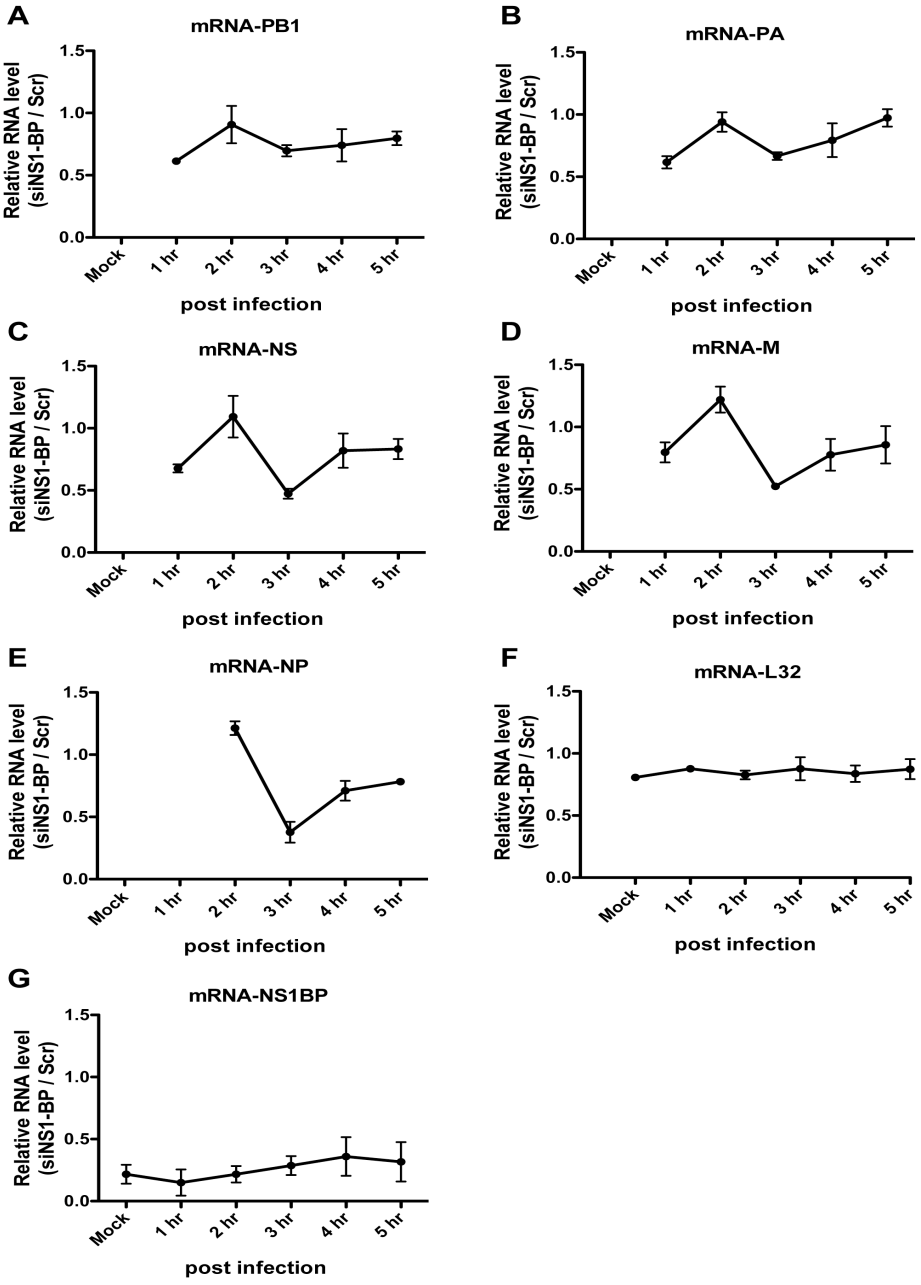

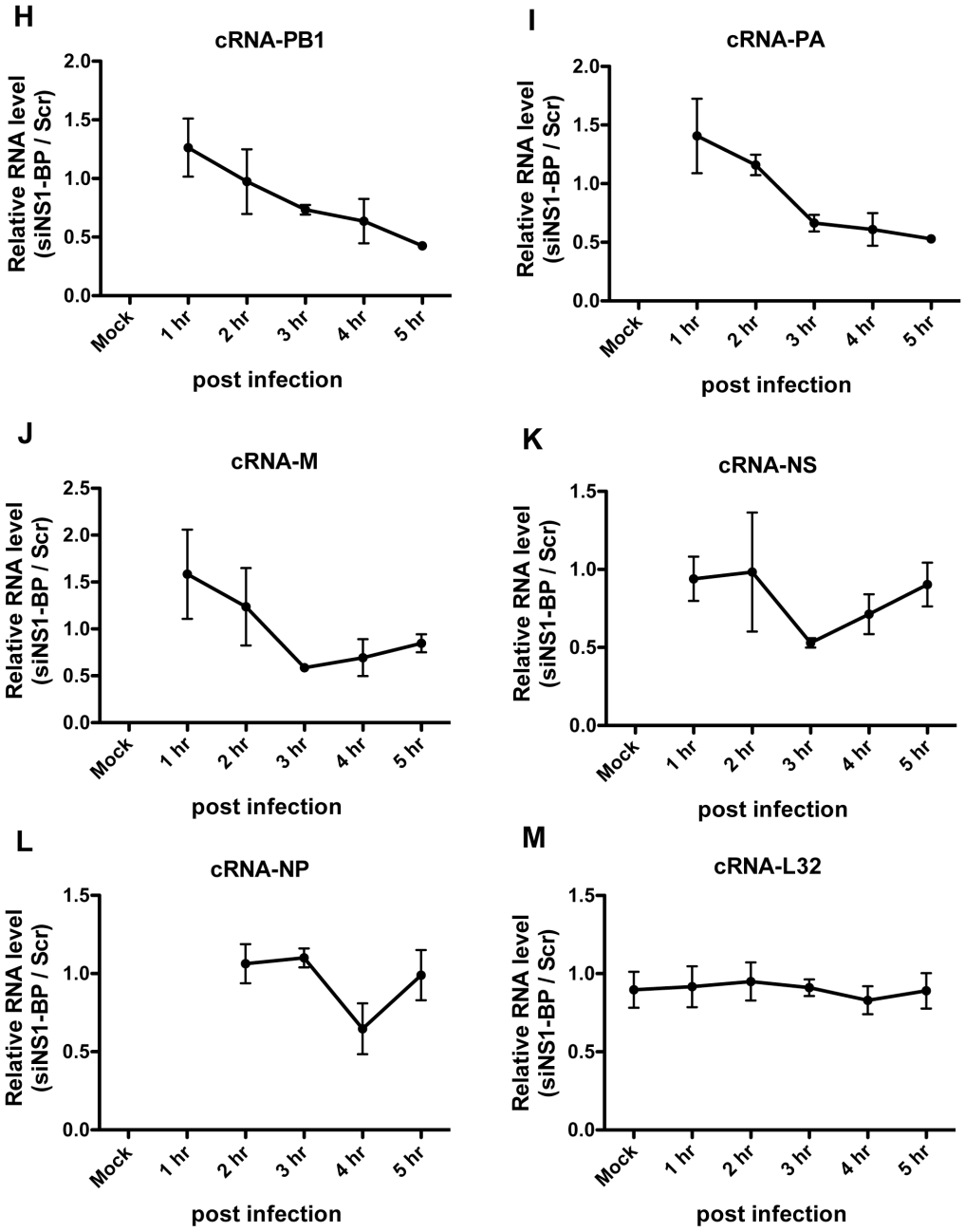
H
cRNA-PB1
Relative RNA level (siNS1-BP / Scr)
2.0
1.5
1.0
0.5
0.0
Mock
1 hr
2 hr
3 hr
4 hr
5 hr
post infection
I
cRNA-PA
Relative RNA level (siNS1-BP / Scr)
2.0
1.5
1.0
0.5
0.0
Mock
1 hr
2 hr
3 hr
4 hr
5 hr
post infection
J
cRNA-M
Relative RNA level (siNS1-BP / Scr)
2.5
2.0
1.5
1.0
0.5
0.0
Mock
1 hr
2 hr
3 hr
4 hr
5 hr
post infection
K
cRNA-NS
Relative RNA level (siNS1-BP / Scr)
1.5
1.0
0.5
0.0
Mock
1 hr
2 hr
3 hr
4 hr
5 hr
post infection
L
cRNA-NP
Relative RNA level (siNS1-BP / Scr)
1.5
1.0
0.5
0.0
Mock
1 hr
2 hr
3 hr
4 hr
5 hr
post infection
M
cRNA-L32
Relative RNA level (siNS1-BP / Scr)
1.5
1.0
0.5
0.0
Mock
1 hr
2 hr
3 hr
4 hr
5 hr
post infection

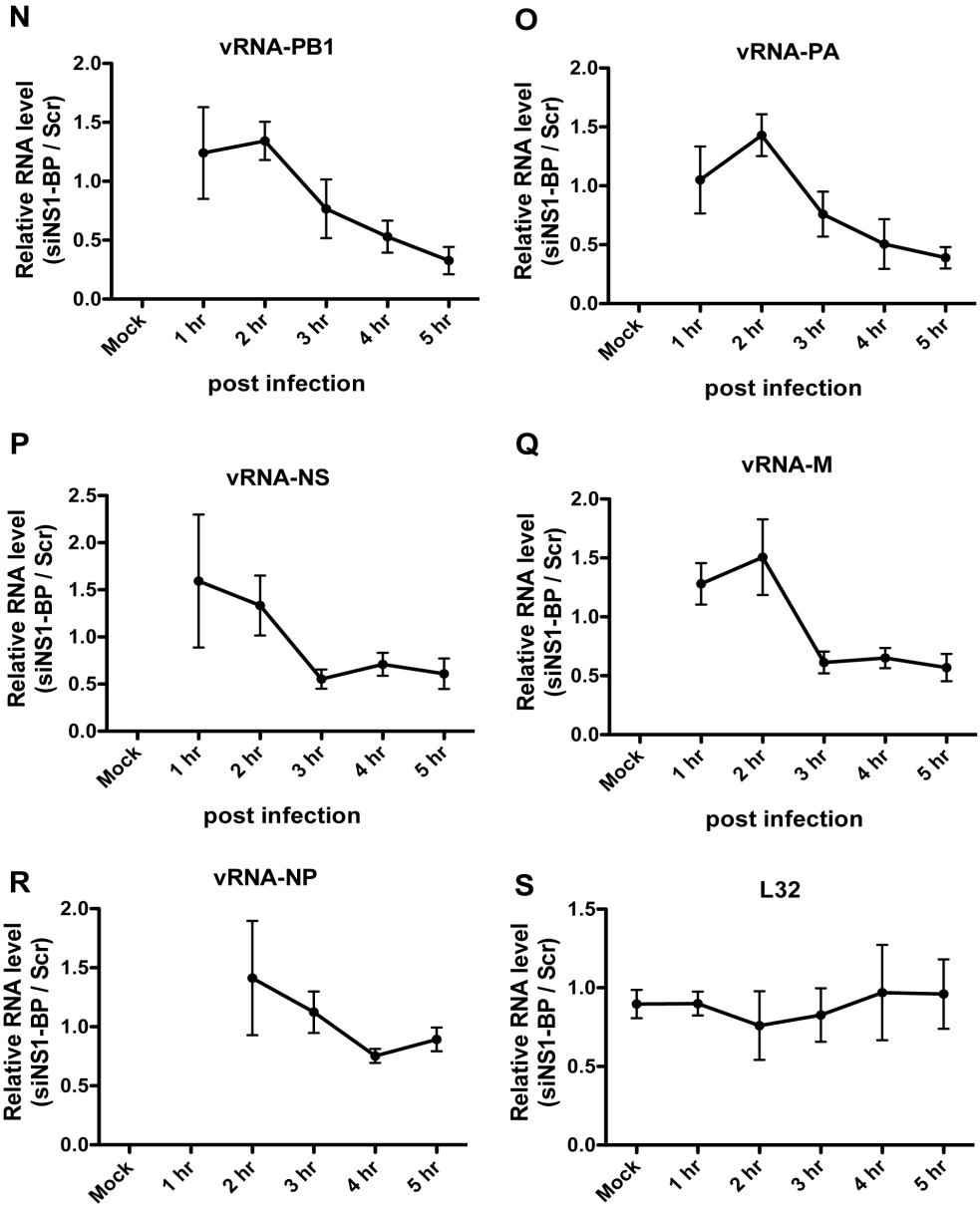

Figure 10. NS1-BP depletion causes the reduced production of viral RNAs. A549 cells were transfected with non-targeting or NS1-BP siRNAs for 48 h and infected with influenza virus at MOI 2. RNAs were isolated at the indicated time points, and 2 μg of total RNAs were subjected to RT-qCR using viral specific primers. (A)-(G) were mRNA, (H)-(M) were cRNA, and (N)-(S) were vRNA. Results were calculated by comparative Ct method (ΔΔCt) using RPL32 gene as the invariably internal control and

finally presented as a relative level normalized to the RNAs of non-targeting siRNA treatment.

3.7 NS1-BP regulates viral RNA accumulation

We showed that low levels of NS1-BP decreased viral RNA synthesis. Since we examined the level of total viral RNAs, the results we observed may represent an additive effect of transcription and mRNA processing. To further characterize whether NS1-BP regulated viral RNA synthesis at the transcription level, I employed a transcriptional pulse strategy in which 5-ethynyl uridine (EU), an analog of uridine, was incorporated into newly synthesized RNAs upon infection. After isolating total RNA, I subjected the RNAs to a chemical reaction that covalently linked biotin to the EU, and the biotin-EU-labeled RNAs were subsequently purified with streptavidin beads and analyzed by qPCR. In this way, I can monitor the amount of newly synthesized viral RNAs in control and NS1-BP depleted cells. The results showed that viral mRNA synthesis was significantly reduced in NS1-BP depleted cells (~30-50% less than the control) (Figure 11 A-D). This effect was not only observed in viral transcription (mRNA) but also in replication (cRNA and vRNA) (Figure 11 E-H & I-L). Thus, I concluded that NS1-BP depletion decreases viral RNA synthesis.

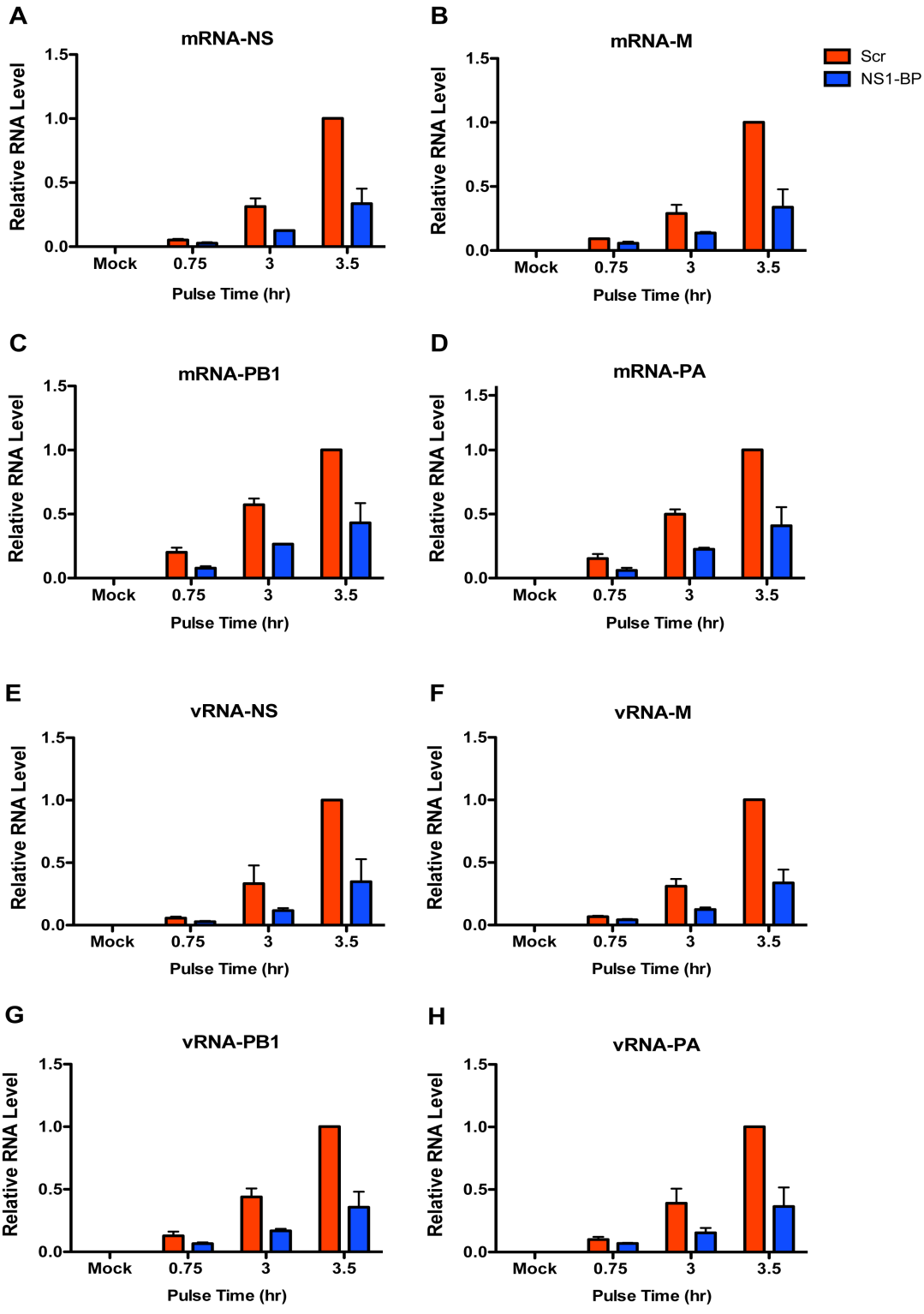
A
mRNA-NS
B
mRNA-M
Scr
NS1-BP
C
mRNA-PB1
D
mRNA-PA
E
vRNA-NS
F
vRNA-M
G
vRNA-PB1
H
vRNA-PA
Relative RNA Level
1.5
1.0
0.5
0.0
Mock
0.75
3
3.5
Pulse Time (hr)

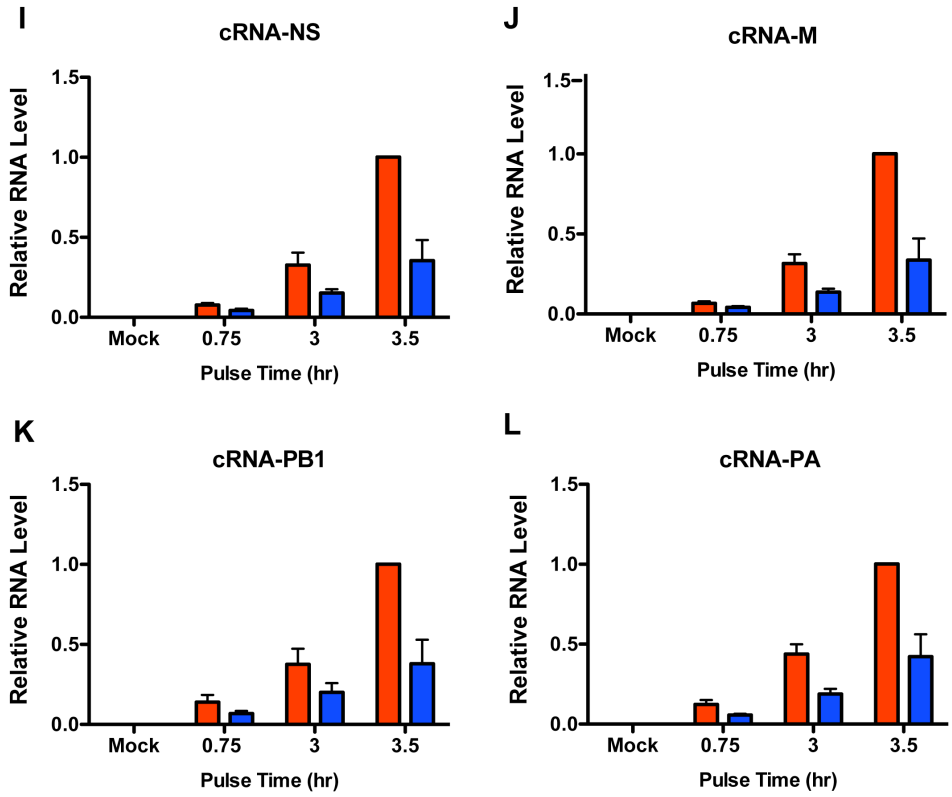

Figure 11. NS1-BP depletion decreases viral RNAs accumulation. A549 cells were treated with 50 μM of non-targeting or NS1-BP siRNAs for 48 h and infected with influenza virus (A/WSN/33) at MOI 2 for 45 min. After washes, cells were incubated in media including 0.5 mM 5-ethynyl uridines (EU) for the indicated times. At each time point, total RNAs were isolated and subjected to a copper-catalyzed reaction with azide-modified biotin. The labeled EU-RNAs were further purified by streptavidin beads and quantified by real time RT-PCR. The Ct number was converted into $2^{(-Ct)}$, and the signal of non-EU treated control was subtracted form the experiments. The result was presented as a relative level normalized to the RNAs of non-targeting siRNA treatment at 3.5 h post infection. (A)-(D) mRNA (E)-(H) vRNA (I)-(L) cRNA. The figure displayed the mean±SD from three independent experiments.

3.8 NS1-BP associates with viral RNA in vivo

Since I showed that NS1-BP was in complex with viral polymerase and regulated viral RNA expression, I then attempted to capture the interaction of NS1-BP with viral RNAs in cells. To study the interaction between protein and RNA, I used a reversible cross-linker that covalently connectes proteins to RNAs within cells. This strategy avoids the re-assortment between proteins and RNAs, which occurs frequently during cell lysis (Conrad, 2008). By crosslinking protein with RNA and applying stringent washing conditions, I could ensure that the Protein-RNA complex I isolated was a bona fide Protein-RNA interaction *in vivo*. Thus, I infected A549 cells with influenza virus at MOI 5 for 5 h, crosslinked the cells with 0.3% formaldehyde, and then lysed the cells with RIPA buffer. The cell lysates were subjected to immunoprecipitation, and the associated viral RNAs were isolated and analyzed by qPCR. Each experiment included three conditions as followed: Immunoprecipitation were performed with NS1-BP antibodies using lysates with or without formaldehyde crosslinking (Figure 12A, lane1 and 2), and control IgG was incubated with lysates subjected to formaldehyde crosslinking (Figure 12A, lane 3). Compared to control IgG (the third lane of each set), NS1-BP immunoprecipitation

significantly pulled down viral RNA segments NS, M, PB1, and PA (Figure 12A). Moreover, this interaction was not restricted to vRNA but also found in viral cRNA and mRNA (Figure 12 B&C). In contrast, there was little detected signal in no-formaldehyde control (the first lane of each set), which reflects that the formaldehyde-dependent signal was a real interaction in cells. Thus, I concluded that NS1-BP associates with viral RNAs *in vivo*. To control the specificity of this assay, I further examined the levels of several housekeeping RNA (GAPDH, β-actin, and α-tubulin), and I did not detect any signal (Figure 12C, right), indicating the specificity of this assay.

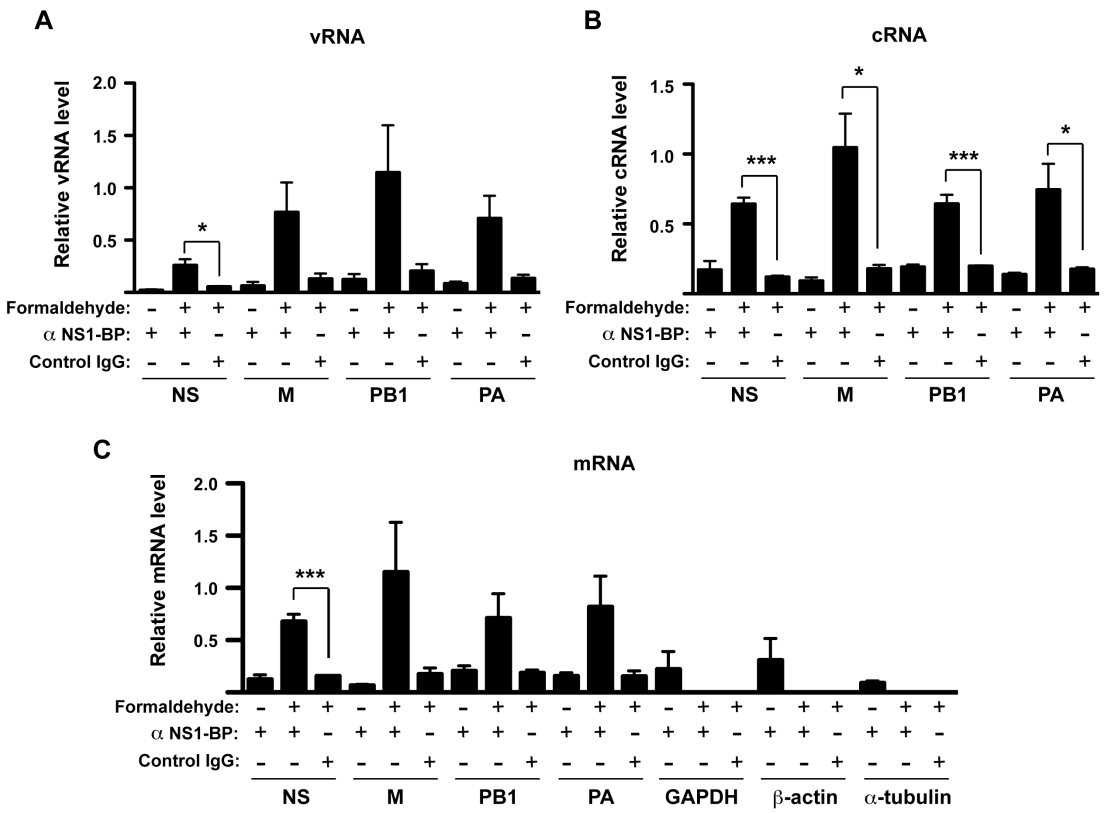

Figure 12. NS1-BP interacts with influenza viral RNAs.
A549 cells were infected with influenza virus at MOI 5 for 5 h and were then cross-linked with 0.3% formaldehyde. Cells were lysed with RIPA buffer, and the lysates were immunoprecipitaed with control IgG or antibodies specific for NS1-BP. After a series of washes, the cross-links were reversed, and the associated RNAs were isolated. Real-time quantitative RT-PCR was used to examine three types of viral RNAs. (A) vRNA, (B) cRAN, and (C) mRNA. Three housekeeping genes (GAPDH, β-actin, and α-tubulin) were included to test the specificity of the assay. The graph displayed the mean±SEM from three independent experiments (*indicates P value <0.05, **indicates P value <0.01, *** indicates P value <0.0001).

3.9 NS1-BP depletion did not affect virus entry

I showed that NS1-BP forms a complex with influenza viral polymerase, and NS1-BP depletion resulted in decreases of viral RNAs, proteins, and replication. The mechanism likely occurs at the transcription level. However, influenza virus replicates its genome in the nucleus; thus, it is also possible that NS1-BP depletion may affect virus entry or vRNP nuclear import, which may generate the same results I have observed. To address this question, I monitored the localization of the influenza nucleoprotein (NP) by immunostaining. If NS1-BP plays a role in virus entry or vRNP nuclear import, it would be expected that the level of NP nuclear localization would decrease in NS1-BP siRNA-depleted cells. However, in both control and NS1-BP-depleted cells, I observed the punctate staining of NP accumulation in the cytoplasm at 1.5 h post infection, suggesting the success of viral entry; moreover, at 2.5 h post infection, the NP signals were detected in the nucleus in both control and NS1-BP depleted cells, indicating that the vRNP was successfully imported to the nucleus (Figure 13A). I quantified the cell number of positive nuclear localization of NP between control and NS1-BP depleted cells at 3 h post infection (ratio of cells with positive NP nuclear

localization to total cell number) and found that NS1-BP depleted cells did not show a significant difference in viral nuclear import compared to the control. The ratio was 0.74 and 0.84 in control and NS1-BP depleted cells, respectively (Figure 13B).

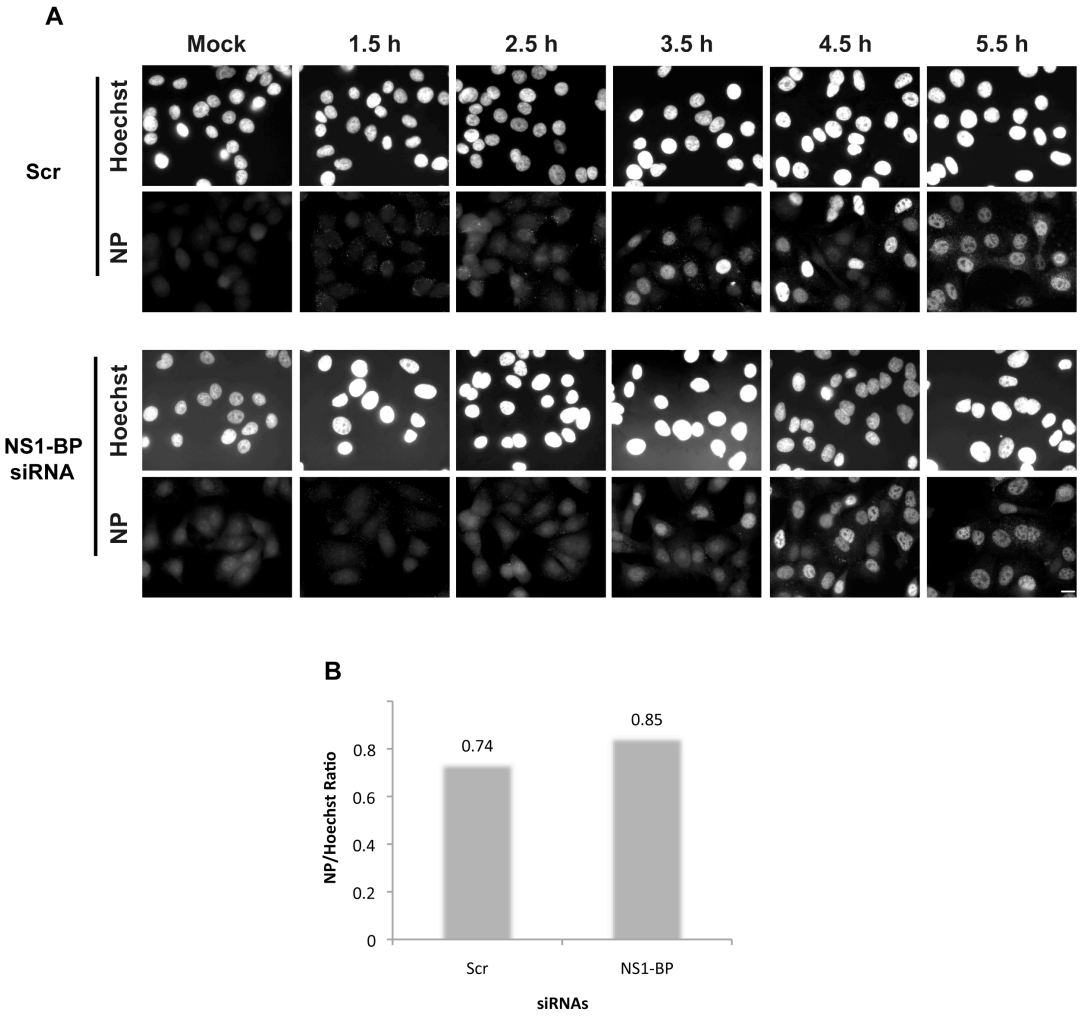

Figure 13. NS1-BP depletion did not affect viral entry.
A549 cells were grown on coverslips, transfected with non-targeting or NS1-BP siRNAs for 48 h, and infected with influenza virus at MOI 10 on ice to synchronize the infection. The cells were then incubated with warm

media and fixed with 3% formaldehyde at each time points as indicated. (A) The cells were stained with Hoechst (Top panel) and antibody against influenza nucleoprotein (bottom panel). Scale bar: 10 μm (B) Quantification of the ratio of NP nuclear localization in non-targeting siRNA or NS1-BP siRNA cells. The ratio was 0.74 and 0.84 in control and NS1-BP depleted cells, respectively.

3.10 NS1-BP did not have effects on cellular splicing

Previous study has suggested that NS1-BP plays a role in pre-mRNA splicing (Wolff et al., 1998). To confirm this function, I employed an *in vivo* mini-genome splicing system as previously described (Rothrock et al., 2003). Minigene CD1 and CD9 constructs used in this assay were derived from gene CD45, a receptor-like tyrosine phosphatase that regulates T cell-mediated signal transduction. CD45 gene includes three variable exons (4, 5, and 6); alternative splicing of these exons results in five different isoforms (Zikherman and Weiss, 2008). The CD1 minigene contains the variable exon 4 that is more susceptible to alternative splicing and flanked by two constitutive exons, termed 3 and 7. In contrast, CD9 minigene includes a constitutive exon 9, which is more resistant to alternative splicing. These minigene constructs encoding transcripts with variable splicing ability were used as substrates to test whether knockdown of NS1-BP has a role in the regulation of splicing. I co-

transfected HeLa cells with the CD1/CD9 minigene plasmid and with non-targeting or NS1-BP siRNAs for 72 h, isolated total RNA, and analyzed the splicing products using low-cycle RT-PCR. Compared to non-targeting siRNA, NS1-BP depletion did not cause significant difference in either splicing or alternative splicing (Figure 14). Thus, it is unlikely that NS1-BP plays a role in pre-mRNA splicing.

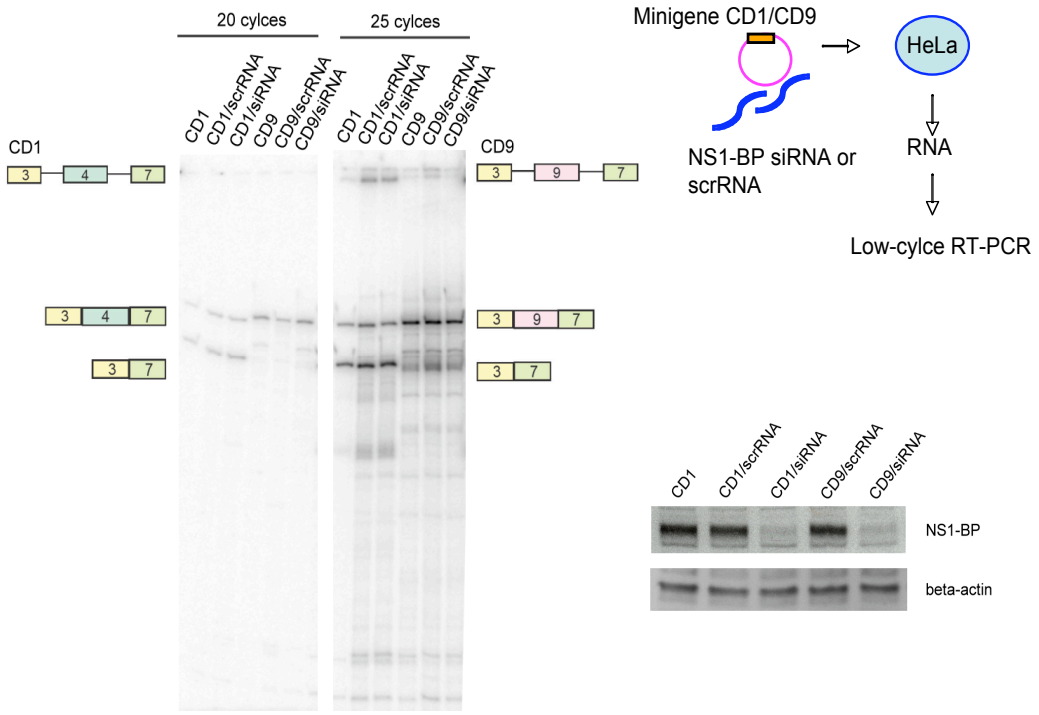

Figure 14. NS1-BP did not appear to be involved in cellular mRNA splicing. (A) HeLa cells were co-transfected with the minigene constructs CD1 or CD9 and with non-targeting siRNA or NS1-BP siRNAs for 72 h. Total RNA was isolated, and 1 μg of RNA was subjected to 20 or 25 cycles of RT-PCR. The corresponding splicing products of CD1 and CD9 minigenes were depicted on the left side and right side, respectively. The signals were quantified using ImageJ and presented as a ratio of three-

exon products to two-exon products. (B) Western blot analysis for knockdown efficiency of NS1-BP siRNAs.

3.11 NS1-BP did not appear to have a role in bulk cellular mRNA export

Since NS1-BP is an RNA binding protein, I next examined whether NS1-BP plays a role in cellular RNA export. I performed oligo-dT *in situ* hybridization to evaluate the distribution of cellular mRNA after 48 h of NS1-BP knockdown. The result showed that there was no obvious difference in the mRNA distribution between the nuclear and cytoplasmic compartments (Figure 15)

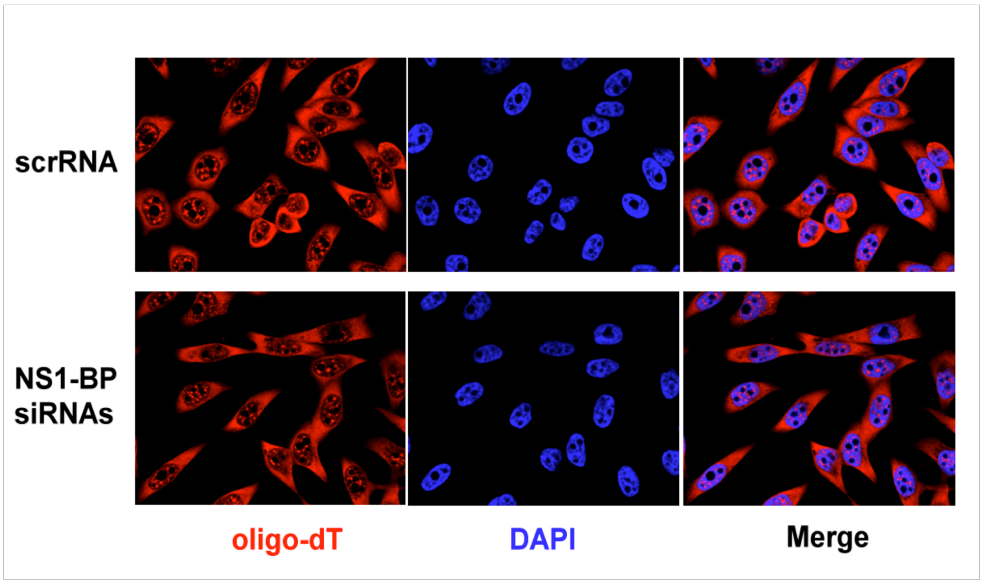

Figure 15. NS1-BP did not play a role in cellular mRNA export.

HeLa cells were grown on coverslips and transfected with non-targeting or NS1-BP siRNA for 48 h. The cells were then fixed with 4% formaldehyde and probed with biotin-labeled oligo-dT followed by Cy3-strepavidin. The blue shows DAPI staining and red shows the distribution of cellular mRNA

CHAPTER FOUR

DISCUSSION

In this study, I discovered three novel properties of the NS1-BP protein. First, NS1-BP interacted with mRNA-binding proteins and the RNA polymerase II, suggesting it is involved in the regulation of gene transcription and/or mRNA processing. Second, NS1-BP associated with the influenza virus polymerase complex and mediated virus RNA synthesis. Third, NS1-BP is an essential factor required for proper viral replication.

NS1-BP was first identified and cloned from a yeast two-hybrid screen as a novel cellular protein that binds to the influenza virus non-structural protein (NS1), and it has been suggested to play a role in pre-mRNA splicing (Wolff et al., 1998). However, over the last decade, there has been little research reported about the functions of NS1-BP, and I speculated that this might be due to the problems of using ectopic overexpression systems to study protein functions. Protein overexpression sometimes results in aggregations or mislocalization, which leads to non-

natural protein-protein interactions, and NS1-BP was such an example. Our results revealed that ectopic expression of NS1-BP caused the artifactual interaction with the chaperone molecule VCP *in vivo*. I then decided to identify the true binding partners of endogenous NS1-BP using immunoprecipitation with specific antibodies, which were generated using the full length GST-NS1-BP as antigen. Although a previous study reported that full length NS1-BP expressed in bacteria was insoluble (Wolff et al., 1998), I found that protein expression at low concentration of IPTG (0.2 mM) and low temperature (20°C) could overcome this problem. Compared to the overexpression system, endogenous NS1-BP co-immunoprecipitated various RNA binding proteins, and VCP was not found in this binding list. Therefore, my study revealed a more appropriate method to examine the functional interacting proteins of NS1-BP.

Most NS1-BP binding partners were RNA binding proteins, such as hnRNPs, DExH/D RNA helicase, cap-binding protein, poly(A) binding proteins, and NFAR. The hnRNPs are a family of proteins associated with nascent mRNA and mediate transcription and/or post-transcriptional events such as pre-mRNA splicing, mRNP assembly, mRNA stability, export, or translation (Han et al., 2010). The DExH/D proteins are a family

of RNA helicases responsible for unwinding RNA duplexes, displacing proteins from protein-RNA complexes (spliceosome assembly), RNP rearrangement, and ribosome biogenesis (Fuller-Pace, 2006; Linder, 2006). Through a search of proteomics studies, I found connections between these RNA-binding proteins and NS1-BP (Fig 16), which indicated that NS1-BP antibodies did not randomly pull down some non-specific cellular proteins; in contrast, it revealed a network, suggesting that NS1-BP was a component of this RNP complex. I further examined whether these interactions were RNA-dependent and found that many of the identified interactions were disrupted in the presence of RNaseA, except for hnRNP M and RNA polymerase II. I did not test all binding proteins, but the results suggested two possibilities for the interactions between NS1-BP and its binding partners. First, NS1-BP itself could be an RNA-binding protein, and thus the RNA binding proteins associated with the same RNAs were pulled down and detected. Although NS1-BP did not contain any known RNA binding motifs, it is not necessary to have the consensus motifs to bind RNA, which has been shown by recent studies (Houmani and Ruf, 2009; Tan et al., 2006; Yeh and Lee, 1995). Another possibility would be that NS1-BP indirectly interacted with these RNA binding proteins, such as RNA polymerase II CTD, which recruites many

factors to its hyperphosphorylated motif during transcription (David et al., 2011; Govind et al., 2010; Phatnani and Greenleaf, 2006). It was difficult for us to demonstrate whether NS1-BP directly bound to RNA, because there was no information regarding RNAs with which NS1-BP might associate and this lack of information increased the difficulty of optimizing the experimental conditions for isolating associated RNAs. To resolve this problem, I am currently trying to identify the associated cellular RNAs using the RIP-Chip assay. Regardless of whether NS1-BP bound RNA directly or indirectly, our data indicated that NS1-BP is a component of an RNP complex. Since NS1-BP associated with the RNA polymerase II CTD in an RNA-independent manner, this further suggested that NS1-BP plays a role in the regulation of gene transcription.

While it is not easy to study the functions of an unknown protein, but viruses can always be used as a good tool to probe gene functions, since they hijack cellular machineries for their own replication. Some of the NS1-BP binding proteins identified here have also been identified in the host-influenza polymerase interactome (Bortz et al., 2011), and viral polymerase activity has been known to dependent on the function of host RNA polymerase II (Engelhardt et al., 2005). Thus, our proteomics

analysis of the NS1-BP interacting partners showed that NS1-BP is in complex with both networks, all of which led us to speculate that NS1-BP might regulate cellular and viral polymerase activity. Luciferase reporter gene assays using the influenza virus promoter were used to examine the effect of NS1-BP depletion on viral polymerase activity, and we showed a reduction of viral polymerase activity upon NS1-BP depletion. Thus, this data suggested that NS1-BP might regulate viral polymerase activity. We have also observed that NS1-BP depletion also caused a reduction in luciferase expression driven by a CMV promoter, which uses host RNA polymerase II. These results suggested a function for NS1-BP in viral and host gene transcription.

Since the readout of the reporter assay driven by the influenza virus protmoter was downstream of transcription, it remained possible that the results of the reporter assays might not result from the regulation of gene transcription but from effects on other post-transcriptional mechanisms. To distinguish these possibilities, I first examined the levels of viral proteins and viral RNAs and found that both decreased in NS1-BP depleted cells. I further employed a transcriptional pulse strategy for a short time period to examine the newly synthesized viral RNAs in control and in NS1-BP

depleted cells. The results indicated that NS1-BP depletion down-regulated viral RNA synthesis at the transcription level. However, there is still the possibility that RNA processing may also account for part of the observed effect as the first measured time points was 45 min after pulse and the experiment lasted for 3.5h. Thus, we sought to exclude that RNA stability was the source of decreased viral RNA expression upon depletion of NS1-BP. There are two ways to examine viral RNA stability *in vivo*: using inhibitors specifically targeted to the viral polymerase or by conducting pulse-chase experiments. First, I used a specific inhibitor (compound 367 identified from small molecule screening (Su et al., 2010) against the virus polymerase PB1 and then monitored the remaining amounts of viral RNAs over time using qPCR. Theoretically, when transcription was stopped, I expected that the viral RNA levels would decrease over time since no new RNA would be synthesized, and the old ones would be degraded. Unfortunately, this compound did not inhibit viral polymerase completely; therefore, the remaining active enzyme kept producing new viral RNAs resulting in increased levels of viral RNAs. Thus, effects of NS1-BP on RNA stability could not be evaluated in this manner. We then tried the pulse-chase experiment approach in which I used 5-ethynyluridine (EU) to label viral RNA for a short period of time and

performed a chase in the presence of excess cold uridine. Surprisingly, the results showed an unexpected increase of viral RNAs over time in both control and NS1-BP depleted cells (data not shown). Where did these labeled EU come from after I washed it away? One possibility was that the increased labeled nucleotides were derived from the cap-snatching mechanism, as influenza virus initiates its transcription by stealing the cap structure from cellular mRNA (Plotch et al., 1981). Alternatively, influenza virus polymerase might have preference for 5-ethynyluridine rather than uridine. Due to the lack of inhibitors of the virus polymerase, it is not possible to use this to examine viral RNA stability *in vivo*.

While we did not directly measure viral RNA stability in NS1-BP depleted cells, we have other evidence indicating that NS1-BP likely regulates viral RNA transcription but not stability. If NS1-BP plays a role in stabilizing viral RNA, this effect would target a specific cis-element. Thus, if I replace the viral RNA sequence with any non-relevant sequence (e.g. Luciferase), I can expect that the effect caused by NS1-BP depletion would disappear, and control and NS-BP knockdown cells should have similar phenotypes. However, in the luciferase assay driven by virus promoter, NS1-BP depletion reduced luciferase synthesis, indicating a

transcriptional regulation but not an effect on RNA stability. Taken together, we concludes that (1) NS1-BP binds Pol II and viral polymerase, (2) low levels of NS1-BP down-regulate viral RNA synthesis; (3) this effects does not occur on RNA stability. These findings strongly indicate a role for NS1-BP as a host factor hijacked by the virus to promote transcription of influenza virus RNAs.

Since viral polymerase activity is dependent on the function of host RNA polymerase II (Engelhardt et al., 2005), I proposed a model in which NS1-BP is a factor that mediates the interactions between cellular RNA polymerase II and the viral polymerase complex during influenza virus infection. Moreover, a recent study also connects some of the NS1-BP binding proteins to viral polymerase activity (Bortz et al., 2011). They select 31 proteins out of host-influenza polymerase interactome that comprise 54 cellular factors associated with the H1N1 influenza polymerase subunits (PB1, PB2, and PA), nucleoprotein (NP), or vRNP (Bortz et al., 2011; Deng et al., 2006; Honda et al., 2007; Jorba et al., 2008; Mayer et al., 2007; Momose et al., 2001; Naito et al., 2007). Using siRNAs together with the influenza mini-genome reporter assay, they define these cellular factors as enhancers or repressors for viral

polymerase activity. Surprisingly, 8 proteins that we found associated with NS1-BP were also identified as enhancers of viral polymerase activity including hnRNPM, hnRNPA1, hnRNP U, RNA polymerase II, Hsp70, Hsp90, PARP1, and DDX17. In contrast, NFAR90 was identified as a repressor. This study extended our results and indicated that influenza virus influenced a connected cellular network for optimizing viral polymerase activity (Figure 16).

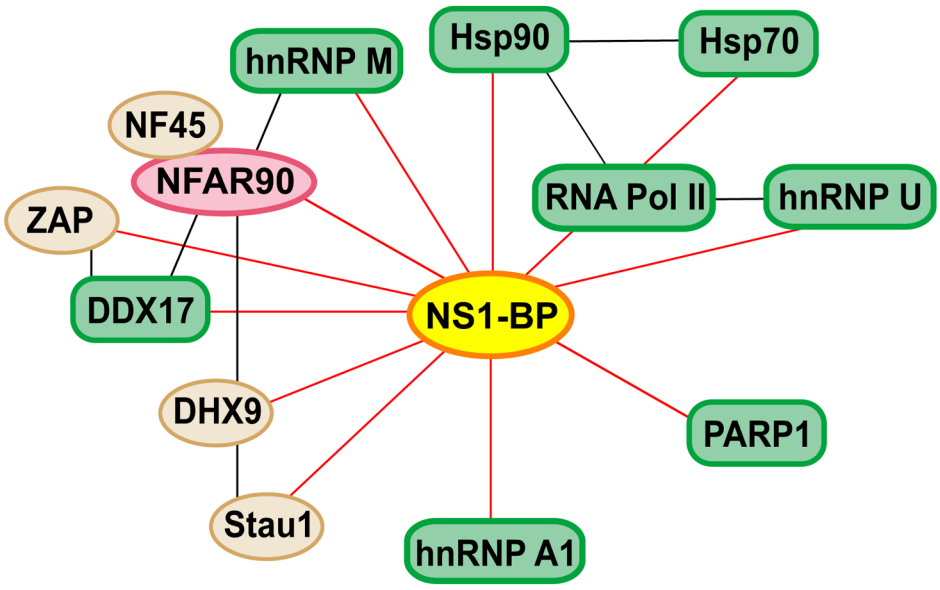

Figure 16. Interaction network of NS1-BP binding proteins.
The diagram represents some of NS1-BP interacting partners identified by mass spectrometry analysis. The red line indicates the interaction with NS1-BP; the black line indicates the interaction between RNA binding proteins. Green circles indicate that the protein is identified as an enhancer of influenza viral polymerase activity (Bortz et al., 2011). The red circle means the suppressor of viral polymerase activity. The brown circles

represent proteins not tested in viral polymerase activity but interact with NS1-BP.

The next question to ask would be what is the function of NS1-BP in host cells? There is little information known about this protein. The co-immunoprecipitation experiments showed that NS1-BP interacted with celluar RNA polymerase II and RNA binding proteins. Using influenza virus as a probe, I demonstrated that NS1-BP regulated viral polymerase activity, and I speculated that NS1-BP might have a similar function in host cells. If NS1-BP regulates cellular transcription, it could be either a general transcription regulator or it could potentially regulate a subset of genes. Since I did not know any transcripts associated with NS1-BP, it becomes difficult to employ the same assay used for virus to study the cellular function of NS1-BP. To overcome this, I analyzed gene expression profile using microarray analysis under NS1-BP depletion. The results showed that NS1-BP depletion did not affect global gene expression; in contrast, three major signature pathways were enriched in differentially expressed genes (unpublished data). These are pathways involved in transcription/mRNA processing, protein translation, and the cell cycle. Some of the functions were consistent with our results of mass spectrometry. Since NS1-BP only regulated specific subsets of genes, it

would be an important direction to identify these genes and their functions in the virus life cycle or in antiviral responses. I can analyze whether there are any common sequences among the promoter regions of these expressed genes, and this may help us uncover the detailed mechanisms and possible transcription factors that may associate with NS1-BP. However, microarray analysis is a downstream readout of gene expression, which includes information resulting from indirect effects of NS1-BP depletion. As for future direction, it will be important to investigate whether NS1-BP has a role in host transcription and identify the genes it regulates.

A previous study showed that NS1-BP co-localizes with the spliceosome assembly factor SC35, and the truncated NS1-BP inhibits pre-mRNA splicing *in vitro* (Wolff et al., 1998). To test whether NS1-BP functioned in slicing *in vivo*, I conducted a splicing assay, using minigene constructs encoding artificial transcripts as substrates. However, compared to the control, NS1-BP depletion did not have significant differences in either splicing or alternative splicing. Although *in vivo* splicing assay is more convincing, I cannot conclude that NS1-BP does not have a role in pre-mRNA splicing, since it remains possible that the negative results might be due to the use of artificial substrates. Therefore,

I need more information regarding gene functions of NS1-BP, and it might be a better idea to test this function once I identify some of the RNAs directly regulated by NS1-BP.

In addition to the cellular splicing assay, I further examined whether NS1-BP depletion affected viral RNA splicing. In the viral genome, M and NS segments generate splicing products. I analyzed viral splicing using qPCR and calculated the splicing effects as a ratio of NS2/NS1 and M2/M1, respectively. In NS segment, there was no obvious ratio change compared to the siRNA control. However, for the M segment, M2/M1 ratio decreased two folds upon NS1-BP depletion during 6 h to 12 h post infection (data not shown). It seems that NS1-BP may regulate M2 splicing.

Another interesting question is whether the non-structural protein (NS1) of influenza virus, together with NS1-BP, regulates viral polymerase activity. NS1 has been shown to interact with the viral polymerase complex in recent studies (Kuo and Krug, 2009; Marion et al., 1997; Robb et al., 2011; Shapira et al., 2009), but whether NS1 regualtes viral polymerase activity remains unknown. To address this question, I might use mutant virus lacking NS1 (ΔNS1) to examine the function of NS1 in viral polymerase activity in future studies.

Significance

In this study, I discovered that the cellular protein NS1-BP is an essential factor hijacked by influenza virus to promote its own replication. NS1-BP binds the viral polymerae, and NS1-BP depletion results in reduced viral polymerase activity. NS1-BP binding proteins have recently been identified as enhancers of viral polymerase activity, which suggested that the influenza virus polymerase might engage cellular protein complex to fulfill its maximum activity, as in the case of NS1-BP. Regarding cellular functions, NS1-BP interacts with RNA polymerase II and other RNA binding proteins, suggesting a function in gene transcription and/or mRNA processing. Gene expression profiling and proteomics analysis indicate that NS1-BP regulates a subsets of cellualr mRNAs involved in transcription/mRNA processing, translation, and the cell cycle. Since NS1-BP is a key contributor to the replication of influenza virus, revealing functions of NS1-BP may have important implications for antiviral therapy.

Tables

Table1. qPCR primer sequences

Targets	Sequences (5'→3')
18S rRNA	Forward: ACCGCAGCTAGGAATAATGGA Reverse: GCCTCAGTTCCGAAAACCA
RPL32	Forward: CGGCGTGCAACAAATCTTACTGTGCCG Reverse: CCAGTTGGGCAGCTCTTTCC
GAPDH	Forward: CGACCGGAGTCAACGGATTTGGTCG Reverse: GGCAACAATATCCACTTTACCAGA
β-actin	Forward: CCGCGAGAAGATGACCCAGAT Reverse: CGTTGGCACAGCCTGGATAGCAACG
α-tubulin	Forward: CACTCTGATTGTGCCTTCATGG Reverse: CGAGCTTAGTGTAGGTTGGGCGCTCG
NS1-BP	Forward: CGCTGGTAATCAACTGGGTGCAGCG Reverse: ACCTCTTCCATCAGCTCTTCCA
PB1	Forward: CGGATTGATGCACGGATTGATTTC Reverse: GACGTCTGAGCTCTTCAATGGTGGAAC
PA	Forward: GCTTCTTATCGTTCAGGCTCTTAGG Reverse: CCGAGAAGCATTAAGCAAAACCCAG
NP	Forward: CTCGTCGCTTATGACAAAGAAG Reverse: AGATCATCATGTGAGTCAGAC
NS	Forward: CAGGACATACTGATGAGGATG Reverse: GTTTCAGAGACTCGAACTGTG
M	Forward: CGCTCAGACATGAGAACAGAATGG Reverse: TAACTAGCCTGACTAGCAACCTC

Table 2. MS data of the associated partners in the absence of RNaseA

Band (kDa)	Accession No.	Protein Name	Score	Theoretical MW (kDa)	No. Masses Matched	Sequence Coverage%
#1	gil4758416	Golgi-specific brefeldin A resistance factor 1	1255	206.3	101	23.6
170-220	gil12667788	Myosin, heavy polypeptide 9, non-muscle	246	226.4	39	14.3
#2	gil17380291	Regulator of nonsense transcripts 1	471	124.3	40	29.2
130-170	gil31621305	Leucine-rich PPR motif-containing protein	421	157.8	39	27.4
	gil100913206	DEAH (Asp-Glu-Ala-His) box polypeptide 9	373	140.9	57	25.7
	gil119582037	La ribonucleoprotein domain family, member 1	203	129.2	35	26.5
	gil4827040	Thyroid hormone receptor associated protein 3	187	108.6	15	14.4
	gil20336290	DEAH (Asp-Glu-Ala-His) box polypeptide 30, isoform 2	173	129.4	19	13.5
#3	gil74136883	Heterogeneous nuclear ribonucleoprotein U isoform a	884	90.5	140	31.8
120-130	gil5762315	Nuclear factor associated with dsRNA NFAR-2	224	95.3	19	18.1
	gil119599167	DEAH (Asp-Glu-Ala-His) box polypeptide 36, isoform CRA_a	210	114.7	17	14.8
	gil119590191	Poly (ADP-ribose) polymerase	188	113.0	12	13.5
#4	gil38201710	DEAD box polypeptide 17 isoform 1	309	80.2	30	26.5
95-120	gil27477136	Zinc finger antiviral protein isoform 1	216	101.4	9	12.2
	gil306891	90kDa heat shock protein	166	83.2	19	17.1
	gil4505343	Nuclear cap binding protein subunit 1, 80kDa	161	91.8	16	14.7
	gil50659095	DEAD (Asp-Glu-Ala-Asp) box polypeptide 21	159	87.3	28	26.9
	gil3319956	E1B-55kDa-associated protein	99	95.8	14	16.7
#5	gi|4504715	Poly(A) binding protein, cytoplasmic 4	607	70.7	73	43.6
72-95	gi|56237027	Insulin-like growth factor 2 mRNA binding protein 1	495	63.4	67	44.9
	gil119589327	Heterogeneous nuclear ribonucleoprotein M, isoform CRA_c	398	77.6	72	40.8
	gil24475847	Influenza virus NS1A binding protein (NS1-BP)	209	71.7	53	24.8
	gil5031755	Heterogeneous nuclear ribonucleoprotein R isoform 2	165	70.9	25	24.5

Band (kDa)	Accession No.	Protein Name	Score	Theoretical MW (kDa)	No. Masses Matched	Sequence Coverage%
#6	gil11527777	Heterogeneous nuclear ribonucleoprotein L	493	60.1	74	42.4
55-72	gil14165437	Heterogeneous nuclear ribonucleoprotein K, isoform a	469	51.0	82	44.4
	gi|5805295	RNA-binding protein isoform G3BP-2a	159	54.1	26	31.1
	gi|4335947	Staufen protein	141	55.0	11	23
#7	gil181486	DNA-binding protein B	644	40.0	43	49.2
45-50	gil14110417	Heterogeneous nuclear ribonucleoprotein D, isoform b	563	36.2	68	37.8
	gil532313	NF45 protein	366	44.7	34	36.5
	gil14249959	Heterogeneous nuclear ribonucleoprotein C (C1/C2)	331	32.4	15	34.1
	gil4826760	Heterogeneous nuclear ribonucleoprotein F	251	45.6	13	25.8
	gil4503571	Enolase 1	234	47.1	13	27.2
	gil3256007	Heterogeneous nuclear ribonucleoprotein G	219	42.4	36	43.7
#8	gil55956921	Heterogeneous nuclear ribonucleoprotein AB isoform b		30.6		
40-45	gil38201714	ELAV-like 1		36.1		
	gil4501885	beta actin		41.7		

BIBLIOGRAPHY

Akarsu, H., Burmeister, W.P., Petosa, C., Petit, I., Muller, C.W., Ruigrok, R.W., and Baudin, F. (2003). Crystal structure of the M1 protein-binding domain of the influenza A virus nuclear export protein (NEP/NS2). EMBO J *22*, 4646-4655.

Baltimore, D. (1971). Expression of animal virus genomes. Bacteriol Rev *35*, 235-241.

Bar-Peled, M., and Raikhel, N.V. (1996). A method for isolation and purification of specific antibodies to a protein fused to the GST. Anal Biochem *241*, 140-142.

Beaton, A.R., and Krug, R.M. (1986). Transcription antitermination during influenza viral template RNA synthesis requires the nucleocapsid protein and the absence of a 5' capped end. Proc Natl Acad Sci U S A *83*, 6282-6286.

Bortz, E., Westera, L., Maamary, J., Steel, J., Albrecht, R.A., Manicassamy, B., Chase, G., Martinez-Sobrido, L., Schwemmle, M., and Garcia-Sastre, A. (2011). Host- and strain-specific regulation of influenza virus polymerase activity by interacting cellular proteins. MBio *2*.

Brownlee, G.G., and Sharps, J.L. (2002). The RNA polymerase of influenza a virus is stabilized by interaction with its viral RNA promoter. J Virol *76*, 7103-7113.

Carver, L.A., Jackiw, V., and Bradfield, C.A. (1994). The 90-kDa heat shock protein is essential for Ah receptor signaling in a yeast expression system. J Biol Chem *269*, 30109-30112.

Chan, S., Choi, E.A., and Shi, Y. (2011). Pre-mRNA 3'-end processing complex assembly and function. Wiley Interdiscip Rev RNA *2*, 321-335.

Chen, W., Calvo, P.A., Malide, D., Gibbs, J., Schubert, U., Bacik, I., Basta, S., O'Neill, R., Schickli, J., Palese, P.*, et al.* (2001). A novel influenza A virus mitochondrial protein that induces cell death. Nat Med *7*, 1306-1312.

Chen, Z., Li, Y., and Krug, R.M. (1999). Influenza A virus NS1 protein targets poly(A)-binding protein II of the cellular 3'-end processing machinery. EMBO J *18*, 2273-2283.

Conrad, N.K. (2008). Chapter 15. Co-immunoprecipitation techniques for assessing RNA-protein interactions in vivo. Methods Enzymol *449*, 317-342.

Cros, J.F., Garcia-Sastre, A., and Palese, P. (2005). An unconventional NLS is critical for the nuclear import of the influenza A virus nucleoprotein and ribonucleoprotein. Traffic *6*, 205-213.

David, C.J., Boyne, A.R., Millhouse, S.R., and Manley, J.L. (2011). The RNA polymerase II C-terminal domain promotes splicing activation through recruitment of a U2AF65-Prp19 complex. Genes Dev *25*, 972-983.

Deng, T., Engelhardt, O.G., Thomas, B., Akoulitchev, A.V., Brownlee, G.G., and Fodor, E. (2006). Role of ran binding protein 5 in nuclear import and assembly of the influenza virus RNA polymerase complex. J Virol *80*, 11911-11919.

Desselberger, U., Racaniello, V.R., Zazra, J.J., and Palese, P. (1980). The 3' and 5'-terminal sequences of influenza A, B and C virus RNA segments are highly conserved and show partial inverted complementarity. Gene *8*, 315-328.

Dias, A., Bouvier, D., Crepin, T., McCarthy, A.A., Hart, D.J., Baudin, F., Cusack, S., and Ruigrok, R.W. (2009). The cap-snatching endonuclease of influenza virus polymerase resides in the PA subunit. Nature *458*, 914-918.

Dunham, E.E., Stevens, E.A., Glover, E., and Bradfield, C.A. (2006). The aryl hydrocarbon receptor signaling pathway is modified through interactions with a Kelch protein. Mol Pharmacol *70*, 8-15.

Engelhardt, O.G., and Fodor, E. (2006). Functional association between viral and cellular transcription during influenza virus infection. Rev Med Virol *16*, 329-345.

Engelhardt, O.G., Smith, M., and Fodor, E. (2005). Association of the influenza A virus RNA-dependent RNA polymerase with cellular RNA polymerase II. J Virol *79*, 5812-5818.

Fechter, P., Mingay, L., Sharps, J., Chambers, A., Fodor, E., and Brownlee, G.G. (2003). Two aromatic residues in the PB2 subunit of influenza A RNA polymerase are crucial for cap binding. J Biol Chem *278*, 20381-20388.

Flick, R., Neumann, G., Hoffmann, E., Neumeier, E., and Hobom, G. (1996). Promoter elements in the influenza vRNA terminal structure. RNA *2*, 1046-1057.

Fuller-Pace, F.V. (2006). DExD/H box RNA helicases: multifunctional proteins with important roles in transcriptional regulation. Nucleic Acids Res *34*, 4206-4215.

Furuta, Y., Takahashi, K., Fukuda, Y., Kuno, M., Kamiyama, T., Kozaki, K., Nomura, N., Egawa, H., Minami, S., Watanabe, Y.*, et al.* (2002). In vitro and in vivo activities of anti-influenza virus compound T-705. Antimicrob Agents Chemother *46*, 977-981.

Furuta, Y., Takahashi, K., Kuno-Maekawa, M., Sangawa, H., Uehara, S., Kozaki, K., Nomura, N., Egawa, H., and Shiraki, K. (2005). Mechanism of action of T-705 against influenza virus. Antimicrob Agents Chemother *49*, 981-986.

Gack, M.U., Albrecht, R.A., Urano, T., Inn, K.S., Huang, I.C., Carnero, E., Farzan, M., Inoue, S., Jung, J.U., and Garcia-Sastre, A. (2009). Influenza A virus NS1 targets the ubiquitin ligase TRIM25 to evade recognition by the host viral RNA sensor RIG-I. Cell Host Microbe *5*, 439-449.

Garcia, M.A., Gil, J., Ventoso, I., Guerra, S., Domingo, E., Rivas, C., and Esteban, M. (2006). Impact of protein kinase PKR in cell biology: from antiviral to antiproliferative action. Microbiol Mol Biol Rev *70*, 1032-1060.

Garcia-Sastre, A., Egorov, A., Matassov, D., Brandt, S., Levy, D.E., Durbin, J.E., Palese, P., and Muster, T. (1998). Influenza A virus lacking the NS1 gene replicates in interferon-deficient systems. Virology *252*, 324-330.

Ge, Q., McManus, M.T., Nguyen, T., Shen, C.H., Sharp, P.A., Eisen, H.N., and Chen, J. (2003). RNA interference of influenza virus production by directly targeting mRNA for degradation and indirectly inhibiting all viral RNA transcription. Proc Natl Acad Sci U S A *100*, 2718-2723.

Geyer, R., Wee, S., Anderson, S., Yates, J., and Wolf, D.A. (2003). BTB/POZ domain proteins are putative substrate adaptors for cullin 3 ubiquitin ligases. Mol Cell *12*, 783-790.

Gibbs, J.S., Malide, D., Hornung, F., Bennink, J.R., and Yewdell, J.W. (2003). The influenza A virus PB1-F2 protein targets the inner mitochondrial membrane via a predicted basic amphipathic helix that disrupts mitochondrial function. J Virol *77*, 7214-7224.

Govind, C.K., Qiu, H., Ginsburg, D.S., Ruan, C., Hofmeyer, K., Hu, C., Swaminathan, V., Workman, J.L., Li, B., and Hinnebusch, A.G. (2010). Phosphorylated Pol II CTD recruits multiple HDACs, including Rpd3C(S), for methylation-dependent deacetylation of ORF nucleosomes. Mol Cell *39*, 234-246.

Guilligay, D., Tarendeau, F., Resa-Infante, P., Coloma, R., Crepin, T., Sehr, P., Lewis, J., Ruigrok, R.W., Ortin, J., Hart, D.J.*, et al.* (2008). The structural basis for cap binding by influenza virus polymerase subunit PB2. Nat Struct Mol Biol *15*, 500-506.

Guo, Z., Chen, L.M., Zeng, H., Gomez, J.A., Plowden, J., Fujita, T., Katz, J.M., Donis, R.O., and Sambhara, S. (2007). NS1 protein of influenza A virus inhibits the function of intracytoplasmic pathogen sensor, RIG-I. Am J Respir Cell Mol Biol *36*, 263-269.

Hale, B.G., Randall, R.E., Ortin, J., and Jackson, D. (2008). The multifunctional NS1 protein of influenza A viruses. J Gen Virol *89*, 2359-2376.

Han, S.P., Tang, Y.H., and Smith, R. (2010). Functional diversity of the hnRNPs: past, present and perspectives. Biochem J *430*, 379-392.

Hastings, J.C., Selnick, H., Wolanski, B., and Tomassini, J.E. (1996). Anti-influenza virus activities of 4-substituted 2,4-dioxobutanoic acid inhibitors. Antimicrob Agents Chemother *40*, 1304-1307.

Hatada, E., Saito, S., and Fukuda, R. (1999). Mutant influenza viruses with a defective NS1 protein cannot block the activation of PKR in infected cells. J Virol *73*, 2425-2433.

Hay, A.J., Lomniczi, B., Bellamy, A.R., and Skehel, J.J. (1977). Transcription of the influenza virus genome. Virology *83*, 337-355.

Hoffmann, E., Stech, J., Guan, Y., Webster, R.G., and Perez, D.R. (2001). Universal primer set for the full-length amplification of all influenza A viruses. Arch Virol *146*, 2275-2289.

Hoffmann, H.H., Palese, P., and Shaw, M.L. (2008). Modulation of influenza virus replication by alteration of sodium ion transport and protein kinase C activity. Antiviral Res *80*, 124-134.

Honda, A., Okamoto, T., and Ishihama, A. (2007). Host factor Ebp1: selective inhibitor of influenza virus transcriptase. Genes Cells *12*, 133-142.

Hornung, V., Ellegast, J., Kim, S., Brzozka, K., Jung, A., Kato, H., Poeck, H., Akira, S., Conzelmann, K.K., Schlee, M.*, et al.* (2006). 5'-Triphosphate RNA is the ligand for RIG-I. Science *314*, 994-997.

Hou, F., Sun, L., Zheng, H., Skaug, B., Jiang, Q.X., and Chen, Z.J. (2011). MAVS forms functional prion-like aggregates to activate and propagate antiviral innate immune response. Cell *146*, 448-461.

Houmani, J.L., and Ruf, I.K. (2009). Clusters of basic amino acids contribute to RNA binding and nucleolar localization of ribosomal protein L22. PLoS One *4*, e5306.

Inoue, A., Kang, M., Fujimura, L., Takamori, Y., Sasagawa, K., Itoh, H., Tokuhisa, T., and Hatano, M. (2005). Overexpression of Nd1-s, a variant form of new kelch family protein, perturbs the cell cycle progression of fibroblasts. DNA Cell Biol *24*, 30-34.

Johnson, N.P., and Mueller, J. (2002). Updating the accounts: global mortality of the 1918-1920 "Spanish" influenza pandemic. Bull Hist Med *76*, 105-115.

Jorba, N., Juarez, S., Torreira, E., Gastaminza, P., Zamarreno, N., Albar, J.P., and Ortin, J. (2008). Analysis of the interaction of influenza virus polymerase complex with human cell factors. Proteomics *8*, 2077-2088.

Kang, M., Matsudo, Y., Sasagawa, K., Tokuhisa, T., and Hatano, M. (2001). Nd1, a novel murine Kelch family protein, may play the role of a housekeeping gene. Biochim Biophys Acta *1519*, 167-174.

Kao, R.Y., Yang, D., Lau, L.S., Tsui, W.H., Hu, L., Dai, J., Chan, M.P., Chan, C.M., Wang, P., Zheng, B.J*., et al.* (2010). Identification of influenza A nucleoprotein as an antiviral target. Nat Biotechnol *28*, 600-605.

Kuo, R.L., and Krug, R.M. (2009). Influenza a virus polymerase is an integral component of the CPSF30-NS1A protein complex in infected cells. J Virol *83*, 1611-1616.

Li, S., Min, J.Y., Krug, R.M., and Sen, G.C. (2006). Binding of the influenza A virus NS1 protein to PKR mediates the inhibition of its activation by either PACT or double-stranded RNA. Virology *349*, 13-21.

Linder, P. (2006). Dead-box proteins: a family affair--active and passive players in RNP-remodeling. Nucleic Acids Res *34*, 4168-4180.

Lu, Y., Wambach, M., Katze, M.G., and Krug, R.M. (1995). Binding of the influenza virus NS1 protein to double-stranded RNA inhibits the activation of the protein kinase that phosphorylates the elF-2 translation initiation factor. Virology *214*, 222-228.

Lynch, K.W., and Weiss, A. (2000). A model system for activation-induced alternative splicing of CD45 pre-mRNA in T cells implicates protein kinase C and Ras. Mol Cell Biol *20*, 70-80.

Marion, R.M., Zurcher, T., de la Luna, S., and Ortin, J. (1997). Influenza virus NS1 protein interacts with viral transcription-replication complexes in vivo. J Gen Virol *78 (Pt 10)*, 2447-2451.

Mata, M.A., Satterly, N., Versteeg, G.A., Frantz, D., Wei, S., Williams, N., Schmolke, M., Pena-Llopis, S., Brugarolas, J., Forst, C.V*., et al.* (2011). Chemical inhibition of RNA viruses reveals REDD1 as a host defense factor. Nat Chem Biol *7*, 712-719.

Mayer, D., Molawi, K., Martinez-Sobrido, L., Ghanem, A., Thomas, S., Baginsky, S., Grossmann, J., Garcia-Sastre, A., and Schwemmle, M. (2007). Identification of cellular interaction partners of the influenza virus ribonucleoprotein complex and polymerase complex using proteomic-based approaches. J Proteome Res *6*, 672-682.

Medina, R.A., and Garcia-Sastre, A. (2011). Influenza A viruses: new research developments. Nat Rev Microbiol *9*, 590-603.

Mercer, J., Schelhaas, M., and Helenius, A. (2010). Virus entry by endocytosis. Annu Rev Biochem *79*, 803-833.

Mibayashi, M., Martinez-Sobrido, L., Loo, Y.M., Cardenas, W.B., Gale, M., Jr., and Garcia-Sastre, A. (2007). Inhibition of retinoic acid-inducible gene I-mediated induction of beta interferon by the NS1 protein of influenza A virus. J Virol *81*, 514-524.

Min, J.Y., and Krug, R.M. (2006). The primary function of RNA binding by the influenza A virus NS1 protein in infected cells: Inhibiting the 2'-5' oligo (A) synthetase/RNase L pathway. Proc Natl Acad Sci U S A *103*, 7100-7105.

Min, J.Y., Li, S., Sen, G.C., and Krug, R.M. (2007). A site on the influenza A virus NS1 protein mediates both inhibition of PKR activation and temporal regulation of viral RNA synthesis. Virology *363*, 236-243.

Momose, F., Basler, C.F., O'Neill, R.E., Iwamatsu, A., Palese, P., and Nagata, K. (2001). Cellular splicing factor RAF-2p48/NPI-5/BAT1/UAP56 interacts with the influenza virus nucleoprotein and enhances viral RNA synthesis. J Virol *75*, 1899-1908.

Nagata, K., Kawaguchi, A., and Naito, T. (2008). Host factors for replication and transcription of the influenza virus genome. Rev Med Virol *18*, 247-260.

Naito, T., Kiyasu, Y., Sugiyama, K., Kimura, A., Nakano, R., Matsukage, A., and Nagata, K. (2007). An influenza virus replicon system in yeast identified Tat-SF1 as a stimulatory host factor for viral RNA synthesis. Proc Natl Acad Sci U S A *104*, 18235-18240.

Nakazawa, M., Kadowaki, S.E., Watanabe, I., Kadowaki, Y., Takei, M., and Fukuda, H. (2008). PA subunit of RNA polymerase as a promising target for anti-influenza virus agents. Antiviral Res *78*, 194-201.

Nayak, D.P., Hui, E.K., and Barman, S. (2004). Assembly and budding of influenza virus. Virus Res *106*, 147-165.

Nemeroff, M.E., Barabino, S.M., Li, Y., Keller, W., and Krug, R.M. (1998). Influenza virus NS1 protein interacts with the cellular 30 kDa subunit of CPSF and inhibits 3'end formation of cellular pre-mRNAs. Mol Cell *1*, 991-1000.

Neumann, G., and Hobom, G. (1995). Mutational analysis of influenza virus promoter elements in vivo. J Gen Virol *76 (Pt 7)*, 1709-1717.

Odagiri, T., Hong, J., and Ohara, Y. (1999). The BM2 protein of influenza B virus is synthesized in the late phase of infection and incorporated into virions as a subviral component. J Gen Virol *80 (Pt 10)*, 2573-2581.

Ohta, Y., Fujimura, L., Nishio, S., Arima, M., Sakamoto, A., Shimada, H., Ochiai, T., Tokuhisa, T., and Hatano, M. (2010). A kelch family protein Nd1-L functions as a metastasis suppressor in cancer cells via Rho family proteins mediated mechanism. Int J Oncol *36*, 427-434.

Opitz, B., Rejaibi, A., Dauber, B., Eckhard, J., Vinzing, M., Schmeck, B., Hippenstiel, S., Suttorp, N., and Wolff, T. (2007). IFNbeta induction by influenza A virus is mediated by RIG-I which is regulated by the viral NS1 protein. Cell Microbiol *9*, 930-938.

Oxford, J., Balasingam, S., and Lambkin, R. (2004). A new millennium conundrum: how to use a powerful class of influenza anti-neuraminidase drugs (NAIs) in the community. J Antimicrob Chemother *53*, 133-136.

Oxford, J.S., Mann, A., and Lambkin, R. (2003). A designer drug against influenza: the NA inhibitor oseltamivir (Tamiflu). Expert Rev Anti Infect Ther *1*, 337-342.

Palese, P., and Shaw, M.L. (2007). Orthomyxoviridae: The virus and their replication, Vol Fields Virology 5th edition (Lippincott Williams & Wilkins, Philadelphia, USA).

Perconti, G., Ferro, A., Amato, F., Rubino, P., Randazzo, D., Wolff, T., Feo, S., and Giallongo, A. (2007). The kelch protein NS1-BP interacts with alpha-enolase/MBP-1 and is involved in c-Myc gene transcriptional control. Biochim Biophys Acta *1773*, 1774-1785.

Perez, J.T., Varble, A., Sachidanandam, R., Zlatev, I., Manoharan, M., Garcia-Sastre, A., and tenOever, B.R. (2010). Influenza A virus-generated small RNAs regulate the switch from transcription to replication. Proc Natl Acad Sci U S A *107*, 11525-11530.

Phatnani, H.P., and Greenleaf, A.L. (2006). Phosphorylation and functions of the RNA polymerase II CTD. Genes Dev *20*, 2922-2936.

Pichlmair, A., Schulz, O., Tan, C.P., Naslund, T.I., Liljestrom, P., Weber, F., and Reis e Sousa, C. (2006). RIG-I-mediated antiviral responses to single-stranded RNA bearing 5'-phosphates. Science *314*, 997-1001.

Pintard, L., Willis, J.H., Willems, A., Johnson, J.L., Srayko, M., Kurz, T., Glaser, S., Mains, P.E., Tyers, M., Bowerman, B.*, et al.* (2003). The BTB protein MEL-26 is a substrate-specific adaptor of the CUL-3 ubiquitin-ligase. Nature *425*, 311-316.

Pinto, L.H., and Lamb, R.A. (1995). Understanding the mechanism of action of the anti-influenza virus drug amantadine. Trends Microbiol *3*, 271.

Plotch, S.J., Bouloy, M., Ulmanen, I., and Krug, R.M. (1981). A unique cap(m7GpppXm)-dependent influenza virion endonuclease cleaves capped RNAs to generate the primers that initiate viral RNA transcription. Cell *23*, 847-858.

Poon, L.L., Fodor, E., and Brownlee, G.G. (2000). Polyuridylated mRNA synthesized by a recombinant influenza virus is defective in nuclear export. J Virol *74*, 418-427.

Poon, L.L., Pritlove, D.C., Fodor, E., and Brownlee, G.G. (1999). Direct evidence that the poly(A) tail of influenza A virus mRNA is synthesized by reiterative copying of a U track in the virion RNA template. J Virol *73*, 3473-3476.

Poon, L.L., Pritlove, D.C., Sharps, J., and Brownlee, G.G. (1998). The RNA polymerase of influenza virus, bound to the 5' end of virion RNA, acts in cis to polyadenylate mRNA. J Virol *72*, 8214-8219.

Randall, R.E., and Goodbourn, S. (2008). Interferons and viruses: an interplay between induction, signalling, antiviral responses and virus countermeasures. J Gen Virol *89*, 1-47.

Robb, N.C., Chase, G., Bier, K., Vreede, F.T., Shaw, P.C., Naffakh, N., Schwemmle, M., and Fodor, E. (2011). The influenza A virus NS1 protein interacts with the nucleoprotein of viral ribonucleoprotein complexes. J Virol *85*, 5228-5231.

Rossman, J.S., Jing, X., Leser, G.P., and Lamb, R.A. (2010). Influenza virus M2 protein mediates ESCRT-independent membrane scission. Cell *142*, 902-913.

Rothrock, C., Cannon, B., Hahm, B., and Lynch, K.W. (2003). A conserved signal-responsive sequence mediates activation-induced alternative splicing of CD45. Mol Cell *12*, 1317-1324.

Sasagawa, K., Matsudo, Y., Kang, M., Fujimura, L., Iitsuka, Y., Okada, S., Ochiai, T., Tokuhisa, T., and Hatano, M. (2002). Identification of Nd1, a novel murine kelch family protein, involved in stabilization of actin filaments. J Biol Chem *277*, 44140-44146.

Satterly, N., Tsai, P.L., van Deursen, J., Nussenzveig, D.R., Wang, Y., Faria, P.A., Levay, A., Levy, D.E., and Fontoura, B.M. (2007). Influenza virus targets the mRNA export machinery and the nuclear pore complex. Proc Natl Acad Sci U S A *104*, 1853-1858.

Schagger, H., and von Jagow, G. (1987). Tricine-sodium dodecyl sulfate-polyacrylamide gel electrophoresis for the separation of proteins in the range from 1 to 100 kDa. Anal Biochem *166*, 368-379.

Schmitt, A.P., and Lamb, R.A. (2005). Influenza virus assembly and budding at the viral budozone. Adv Virus Res *64*, 383-416.

Shapira, S.D., Gat-Viks, I., Shum, B.O., Dricot, A., de Grace, M.M., Wu, L., Gupta, P.B., Hao, T., Silver, S.J., Root, D.E*., et al.* (2009). A physical and regulatory map of host-influenza interactions reveals pathways in H1N1 infection. Cell *139*, 1255-1267.

Sieczkarski, S.B., and Whittaker, G.R. (2002). Influenza virus can enter and infect cells in the absence of clathrin-mediated endocytosis. J Virol *76*, 10455-10464.

Silverman, R.H. (2007). Viral encounters with 2',5'-oligoadenylate synthetase and RNase L during the interferon antiviral response. J Virol *81*, 12720-12729.

Stegmann, T. (2000). Membrane fusion mechanisms: the influenza hemagglutinin paradigm and its implications for intracellular fusion. Traffic *1*, 598-604.

Stogios, P.J., and Prive, G.G. (2004). The BACK domain in BTB-kelch proteins. Trends Biochem Sci *29*, 634-637.

Su, C.Y., Cheng, T.J., Lin, M.I., Wang, S.Y., Huang, W.I., Lin-Chu, S.Y., Chen, Y.H., Wu, C.Y., Lai, M.M., Cheng, W.C.*, et al.* (2010). High-throughput identification of compounds targeting influenza RNA-dependent RNA polymerase activity. Proc Natl Acad Sci U S A *107*, 19151-19156.

Tan, Y.W., Fang, S., Fan, H., Lescar, J., and Liu, D.X. (2006). Amino acid residues critical for RNA-binding in the N-terminal domain of the nucleocapsid protein are essential determinants for the infectivity of coronavirus in cultured cells. Nucleic Acids Res *34*, 4816-4825.

Taubenberger, J.K., and Kash, J.C. (2010). Influenza virus evolution, host adaptation, and pandemic formation. Cell Host Microbe *7*, 440-451.

Tomassini, J., Selnick, H., Davies, M.E., Armstrong, M.E., Baldwin, J., Bourgeois, M., Hastings, J., Hazuda, D., Lewis, J., McClements, W.*, et al.* (1994). Inhibition of cap (m7GpppXm)-dependent endonuclease of influenza virus by 4-substituted 2,4-dioxobutanoic acid compounds. Antimicrob Agents Chemother *38*, 2827-2837.

Umbach, J.L., Yen, H.L., Poon, L.L., and Cullen, B.R. (2010). Influenza A virus expresses high levels of an unusual class of small viral leader RNAs in infected cells. MBio *1*.

Vreede, F.T., Jung, T.E., and Brownlee, G.G. (2004). Model suggesting that replication of influenza virus is regulated by stabilization of replicative intermediates. J Virol *78*, 9568-9572.

Wang, Q., Song, C., and Li, C.C. (2004). Molecular perspectives on p97-VCP: progress in understanding its structure and diverse biological functions. J Struct Biol *146*, 44-57.

Wise, H.M., Foeglein, A., Sun, J., Dalton, R.M., Patel, S., Howard, W., Anderson, E.C., Barclay, W.S., and Digard, P. (2009). A complicated message: Identification

of a novel PB1-related protein translated from influenza A virus segment 2 mRNA. J Virol *83*, 8021-8031.

Wolff, T., O'Neill, R.E., and Palese, P. (1998). NS1-Binding protein (NS1-BP): a novel human protein that interacts with the influenza A virus nonstructural NS1 protein is relocalized in the nuclei of infected cells. J Virol *72*, 7170-7180.

Wright, P.F., Neumann, G., and Kawaoka, Y. (2007). Orthomyxoviruses, Vol Fields Virology 5th edn (Lippincott Williams & Wilkins, Philadelphia, USA).

Xu, L., Wei, Y., Reboul, J., Vaglio, P., Shin, T.H., Vidal, M., Elledge, S.J., and Harper, J.W. (2003). BTB proteins are substrate-specific adaptors in an SCF-like modular ubiquitin ligase containing CUL-3. Nature *425*, 316-321.

Yeh, L.C., and Lee, J.C. (1995). Contributions of multiple basic amino acids in the C-terminal region of yeast ribosomal protein L1 to 5 S rRNA binding and 60 S ribosome stability. J Mol Biol *246*, 295-307.

Yuan, P., Bartlam, M., Lou, Z., Chen, S., Zhou, J., He, X., Lv, Z., Ge, R., Li, X., Deng, T.*, et al.* (2009). Crystal structure of an avian influenza polymerase PA(N) reveals an endonuclease active site. Nature *458*, 909-913.

Zamarin, D., Garcia-Sastre, A., Xiao, X., Wang, R., and Palese, P. (2005). Influenza virus PB1-F2 protein induces cell death through mitochondrial ANT3 and VDAC1. PLoS Pathog *1*, e4.

Zheng, H., Lee, H.A., Palese, P., and Garcia-Sastre, A. (1999). Influenza A virus RNA polymerase has the ability to stutter at the polyadenylation site of a viral RNA template during RNA replication. J Virol *73*, 5240-5243.

Zikherman, J., and Weiss, A. (2008). Alternative splicing of CD45: the tip of the iceberg. Immunity *29*, 839-841.

Zollman, S., Godt, D., Prive, G.G., Couderc, J.L., and Laski, F.A. (1994). The BTB domain, found primarily in zinc finger proteins, defines an evolutionarily conserved family that includes several developmentally regulated genes in Drosophila. Proc Natl Acad Sci U S A *91*, 10717-10721.